Title
Identifying Neural Mechanisms of Aberrant Salience and Inhibitory Processing in Patients with Schizophrenia

Author
Guha, Anika Maya

Publication Date
2022

Peer reviewed|Thesis/dissertation

UNIVERSITY OF CALIFORNIA

Los Angeles

Identifying Neural Mechanisms of Aberrant Salience and Inhibitory Processing in Patients with Schizophrenia

A dissertation submitted in partial satisfaction of the requirements for the degree Doctor of Philosophy in Psychology

by

Anika Maya Guha

2022

ABSTRACT OF THE DISSERTATION

Identifying Neural Mechanisms of Aberrant Salience and Inhibitory Processing in Patients with Schizophrenia

by

Anika Maya Guha

Doctor of Philosophy in Psychology

University of California, Los Angeles, 2022

Professor Cindy M. Yee-Bradbury, Co-Chair

Professor Gregory Allen Miller, Co-Chair

Individuals with schizophrenia (SZ) commonly demonstrate attentional deficits, which in turn may contribute to higher-level cognitive dysfunction and clinical symptoms associated with the disorder. In EEG studies, these deficits are reliably observed during an auditory paired-stimulus paradigm, in which two identical stimuli are presented 500 ms apart. Relative to healthy comparison participants (HC), SZ typically exhibit a smaller N100 component of the event-related brain potential (ERP) following the first stimulus, indicative of impaired allocation of attention. HC generally demonstrate a decrease in N100 amplitude in response to the second stimulus relative to the first (i.e., N100 suppression), whereas SZ reliably demonstrate less suppression, indicative of inhibitory filtering dysfunction. A separate body of research using

fMRI has linked salience and inhibitory processing deficits in SZ to insufficient suppression of the default mode network (DMN) of the brain, which supports internally-based processes and self-referential processing. The salience network (SAL), a higher-order system responsible for monitoring stimulus salience, regulates DMN as needed for tasks requiring attention to external stimuli. Given the shared constructs associated with N100 responses and the connectivity between DMN and SAL, it was hypothesized that these N100 variables and neural network measures capture disorder-related dysfunction in shared mechanisms of salience and inhibitory processing and would thus be related. To evaluate these relationships in SZ (N = 52) and HC (N = 25), a multimodal approach was employed using resting-state fMRI, resting-state EEG, and EEG recorded during the paired-stimulus paradigm. Among SZ, resting state hyperconnectivity within DMN was observed using both oscillatory EEG and fMRI data, with DMN hyperconnectivity observed specifically in the EEG beta frequency band. SZ and HC generally demonstrated opposing relationships between resting state DMN connectivity and N100 variables, such that greater intra-DMN connectivity was associated with attenuated N100 amplitude and higher N100 ratio scores in SZ. SZ also demonstrated greater resting state DMN-to-SAL effective connectivity than SAL-to-DMN connectivity, whereas HC demonstrated no such asymmetry. In oscillatory EEG collected during the paired-stimulus paradigm, SZ demonstrated less evoked theta-band connectivity within DMN following presentation of the auditory stimulus. No relationships between task-based network connectivity measures and N100 variables were identified. Present findings demonstrate specific profiles of DMN dysfunction in SZ that differentially relate to attentional processes indexed by measures obtained from the N100 ERP component during the paired-stimulus paradigm. Multimodal data fusion demonstrated that EEG and fMRI assessments of DMN were related yet also captured unique aspects of network

function associated with N100 phenomena in SZ. Future work can build upon this research to further clarify how alterations in these neural mechanisms contribute to disorder-related impairments and inform promising targets for individualized prevention and treatment.

The dissertation of Anika Maya Guha is approved.

Katherine H. Karlsgodt

Keith H. Nuechterlein

Cindy M. Yee-Bradbury, Committee Co-Chair

Gregory Allen Miller, Committee Co-Chair

University of California, Los Angeles

2022

TABLE OF CONTENTS

LIST OF TABLES AND FIGURES

ACKNOWLEDGEMENTS

This work was supported by a UCLA Graduate Division Dissertation Year Fellowship and National Institute of Mental Health (NIMH) F31 MH124421-01 awarded to Anika Maya Guha, and NIMH R01 MH110544 (MPIs: Cindy Yee-Bradbury, PhD, Gregory A. Miller, PhD, Keith Nuechterlein, PhD). I also gratefully acknowledge the patients and staff of the UCLA Aftercare Research Program for their important contributions.

Anika Maya Guha

EDUCATION

2017 - present	**University of California, Los Angeles** Doctor of Philosophy, Expected 2022 Advisors: Gregory A. Miller, Ph.D., Cindy Yee-Bradbury, Ph.D.
December 2017	**University of California, Los Angeles** Master of Arts, Clinical Psychology Advisors: Gregory A. Miller, Ph.D., Cindy Yee-Bradbury, Ph.D. Thesis: Hyperactivity in Broca's area as a moderator of top-down control in depression and anxiety.
May 2014	**Wellesley College** Bachelor of Arts, *cum laude,* Neuroscience with Minor in Psychology Research Advisor: Jeremy Wilmer, Ph.D. Thesis: Effects of action video game training on multiple object tracking and mental rotation abilities.

GRANTS AND FELLOWSHIPS

2021	National Research Service Award Predoctoral Fellowship (F31 MH124421-01), NIMH ($86,124)
2020	Dissertation Year Fellowship, UCLA ($20,000)
2018	Graduate Summer Research Mentorship Award, UCLA ($6,000)
2017	Graduate Summer Research Mentorship Award, UCLA ($6,000)
2016	Edwin W. Pauley Fellowship, UCLA ($15,000)
2016	Department of Psychology Fellowship, UCLA ($21,000)

AWARDS AND HONORS

2020	Clinical Service Award, UCLA ($500)
2019	Student Poster Award, Society for Psychophysiological Research ($300)
2017 – 2020	Letters of Clinical Excellence, UCLA Psychology Clinic
2014	Cum Laude Latin Honors, Wellesley College
2014	Sigma Xi Scientific Research Society

PUBLICATIONS

Guha, A., Yee, C. M., Heller, W., & Miller, G. A. (2021). Alterations in the default mode-salience network circuit provide a potential mechanism supporting negativity bias in depression. *Psychophysiology*, 00, e13918. https://doi.org/10.1111/psyp.13918

Edgar, J.C., **Guha, A.**, & Miller, G.A. (2020). Magnetoencephalography for schizophrenia. Special issue on magnetoencephalography, R.R. Lee & M.X. Huang (Eds.), *Neuroimaging Clinics, 30,* 205-216.

Kalonji, C., Wenger, D., **Guha, A**., Yarosh, C., Koney, N., Hoffman, C. (In press). Educating patients on nutrition using a short computer-based video: A successful clinic model. *International Journal of Disease Reversal and Prevention.*

Fisher, J., **Guha, A.**, Heller, W., Miller, G.A. (2019). Extreme-groups designs in studies of dimensional phenomena: Advantages, caveats, and recommendations. *Journal of Abnormal Psychology, 129*, 14-20. dx.doi.org/10.1037/abn0000480.

Guha, A., Spielberg, J., Lake, J., Popov, T., Heller, W., Yee, C.M., & Miller, G.A. (2019). Effective connectivity between Broca's area and amygdala as a mechanism of top-down control in worry. *Clinical Psychological Science, 7*. doi: 10.1177/2167702619867098.

Fritz, T., Mueller, K., **Guha, A.**, Gouws, A., Levita, L., Andrews, T. J., & Slocombe, K. E. (2018). Human behavioural discrimination of human, chimpanzee and macaque affective vocalisations is reflected by the neural response in the superior temporal sulcus. *Neuropsychologia*, 111, 145-150.

Smith, R. X., **Guha, A**., Vaida, F., Paul, R. H., & Ances, B. (2017). Prefrontal recruitment mitigates risk-taking behavior in human immunodeficiency virus-infected young adults. *Clinical Infectious Diseases*, 66(10), 1595-1601.

Guha, A., Brier, M. R., Ortega, M., Westerhaus, E., Nelson, B., & Ances, B. M. (2016). Topographies of cortical and subcortical volume loss in HIV and aging in the cART era. *JAIDS Journal of Acquired Immune Deficiency Syndromes*, 73(4), 374-383.

Guha, A., Wang, L., Tanenbaum, A., Esmaeili-Firidouni, P., Wendelken, L. A., Busovaca, E., ... & Valcour, V. (2016). Intrinsic network connectivity abnormalities in HIV-infected individuals over age 60. *Journal of Neurovirology*, 22(1), 80-87.

Fritz, T. H., Ciupek, M., Kirkland, A., Ihme, K., **Guha, A.,** Hoyer, J., & Villringer, A. (2014). Enhanced response to music in pregnancy. *Psychophysiology*, 51(9), 905-911.

RESEARCH EXPERIENCE

August 2016 – Present	**University of California, Los Angeles** Ph.D. student researcher, Laboratory for Clinical and Affective Psychophysiology Advisors: Gregory A. Miller, Ph.D., and Cindy Yee-Bradbury, Ph.D.
July 2014 – August 2016	**Washington University School of Medicine in St. Louis** Research assistant and data analyst, Neurology Department Supervisor: Beau Ances, M.D., Ph.D.
May 2013 – August 2014	**Wellesley College** Student researcher, Human Variation Laboratory Advisor: Jeremy Wilmer, Ph.D.
June 2012 – August 2012	**Max-Planck-Institute for Human Cognitive and Brain Sciences** Research Intern, Cognitive Neurology Department Supervisor: Thomas Fritz, Ph.D.

CLINICAL EXPERIENCE

2021 – 2022	**West Los Angeles VA Medical Center** Psychology Intern
2017 - 2021	**UCLA Psychology Clinic** Neuropsychology Assessor, Intake Clinician, Graduate Student Therapist, Peer Supervisor
2018 – 2019	**CBT for Psychosis Clinic, West Los Angeles VA Medical Center** Psychology Pre-Intern

General Introduction

Schizophrenia is a severe psychiatric disorder characterized by significant cognitive dysfunction. In turn, cognitive deficits in patients diagnosed with schizophrenia (SZ) are associated with diverse clinical symptoms and predict poor overall functional outcome (e.g. Bowie & Harvey, 2006). Within the domain of cognitive processing, considerable evidence suggests that filtering of information and allocation of attention are consistently disrupted in the disorder (Gjini et al., 2011; Gold et al., 2018; Kopp et al., 1994; Luck et al., 2019; Sawaki et al., 2017) and appear to covary with clinical symptom ratings and other areas of cognitive performance (e.g., Hamilton et al., 2008; Smith et al., 2011; Yee et al., 1998). Research aimed at evaluating the neural mechanisms associated with cognitive processing dysfunction in SZ has been somewhat segregated by neuroimaging modality, despite purporting to investigate shared constructs. Using EEG and fMRI data fusion, the present dissertation was designed to examine communication within and between two networks of interacting brain regions to determine how disruptions in salience monitoring and inhibitory processing are associated with dysfunction in SZ. This multimodal approach enhances characterization of mechanisms of abnormal cognitive processing in SZ .

N100 in Schizophrenia

One line of research examining disruption of cognitive processes in SZ utilizes the N100 component of the event-related brain potential (ERP) to evaluate the deployment of attention. Healthy comparison subjects (HC) typically demonstrate N100 suppression during the "paired-stimulus" paradigm, in which two identical auditory stimuli are presented 500 ms apart. Because the second stimulus (S2) conveys identical information associated with the first stimulus (S1), HC generally demonstrate a decrease in the amplitude of the auditory N100 component of the

event-related potential (ERP), occurring ~100 ms after stimulus onset, in response to S2 compared to S1 (e.g., Boutros et al., 2009). Suppression of N100 amplitude to S2 is postulated to reflect an inhibitory filtering mechanism that is activated by S1 to prevent sensory overload, particularly to redundant information, and to protect the integrity of higher-order cognitive functions (Smith et al., 2010; Rosburg, 2018). SZ have been found to exhibit aberrant N100 responses during the paired-stimulus paradigm, including a smaller N100 to S1 and N100 suppression deficits (Boutros, Korzyukov, Jansen, Feingold, & Bell, 2004; Smith et al., 2010; Turetsky et al., 2008). Whereas N100 suppression is thought to reflect inhibition of redundant sensory input associated with S2 thus "gating out" irrelevant information, attenuation of N100 amplitude to S1 in SZ may reflect impaired allocation of attention to the initial stimulus thus "gating in" important information (Boutros & Belger, 1999). The two deficits need not occur together and may reflect distinct aspects of the pathophysiology associated with SZ.

Using a ratio score of S2/S1 to assess degree of N100 suppression, findings from multiple investigations indicate that higher ratio scores in SZ may primarily reflect smaller N100 amplitude to S1, corresponding to impaired attention, rather than a suppression deficit involving S2 (Connolly et al., 1985; Roth et al., 1980, 1991; Saletu et al., 1971; Shagass et al., 1978; Todd et al., 2000). In line with this hypothesis, a recent meta-analysis revealed that reductions in N100 to S1 in SZ are more reliably observed than N100 suppression deficits (Rosburg, 2018). However, several other studies have demonstrated consistent N100 suppression deficits in SZ (Boutros et al., 2019; Lijffijt et al., 2009; Brockhaus-Dumke et al., 2008).

Evaluation of both N100 amplitude to S1 and the N100 ratio score enables the investigation of the encoding and orientation processes captured by the response to S1 as well as the attentional filtering captured by the response to S2. In combination, consideration of abnormal

N100 responses in SZ provides a valuable means of substantiating misattribution of salience as a mediating mechanism between a variety of neurocognitive findings and psychotic symptoms, such as delusions and hallucinations (Hare et al., 2019; Howes & Murray, 2014; Palaniyappan & Liddle, 2012; Winton-Brown et al., 2014)

Salience Processing

Salience processing corresponds to the evaluation of incoming information for salience and selection of information for additional processing (Menon, 2015) and is thought to determine attentional selection (Tsakanikos, 2004). It has been suggested that aberrant salience, attached to internal cognitions and events (e.g., inner speech), and deficits in source monitoring (e.g., corollary discharge; Ford & Mathalon, 2005) both contribute to "self-disturbance," or the sense that an individual is not the source of their own thoughts and actions (De Vries et al., 2013), and related psychotic symptoms (e.g., auditory hallucinations) in SZ. However, it remains unclear whether these processes are aspects of the same neurocognitive mechanism or whether one predicts downstream effects of the other (Nelson et al., 2014b, 2014a).

Neural Networks

Identification of crucial neural network dynamics may bridge some gaps in current conceptualizations of filtering, salience processing, and early attention deficits associated with SZ. In a body of research largely distinct from that utilizing ERPs, numerous studies using functional magnetic resonance imaging (fMRI) have demonstrated abnormal connectivity of neural networks in SZ. Dysfunction of two major brain networks, the default mode (DMN) and salience (SAL) networks, appear to contribute to a mechanism supporting salience processing and attentional deficits in the disorder (Manoliu et al., 2014; Orliac et al., 2013; Wotruba et al., 2014).

Default Mode Network

DMN refers to a large-scale brain network of interacting regions most highly correlated with one another at wakeful rest. Although conceptualization of DMN continues to evolve, prevailing theories suggest that DMN supports computations that enable self-referential processing, including mentation and daydreaming (Buckner et al., 2008). Because this set of functions contrasts with goal-directed processing, effective suppression of DMN is often important during cognitive processing of external stimuli in order to disengage from distracting internal processes (Anticevic et al., 2012; L. Zhou et al., 2016). In fact, several studies with HC have found that lower DMN activity is associated with more successful performance on experimental tasks assessing attention (Weissman et al., 2006) and working memory (Anticevic et al., 2010).

DMN suppression may additionally support disengagement from distracting, externally-generated information. For example, Chadick and Gazzaley (2011) manipulated task-relevant vs. task-irrelevant visual distraction during a test of working memory and examined connectivity between the DMN and stimulus-selective visual regions. Greater connectivity between DMN and stimulus-selective visual regions was observed only in the presence of task-irrelevant distraction, when activity in visual regions was being suppressed, such that less DMN activation was accompanied by less activation in visual regions associated with task-irrelevant processing. Additionally, trial-by-trial DMN activity negatively predicted reaction time on the task, such that reduced DMN was associated with faster performance, and DMN-to-visual region connectivity was associated with faster responses in the presence of task-irrelevant distraction. These findings suggest that DMN plays an important role in the suppression of externally-generated distraction as well as suppression of distracting, introspective cognitive processes.

Default Mode Network in Schizophrenia

Multiple studies have demonstrated abnormal intra-network DMN connectivity in SZ (for a review, see Hu et al., 2017). Resting-state fMRI (rs-fMRI) studies most commonly observe DMN hyperconnectivity in SZ (Garrity et al., 2007; Jafri et al., 2008; Y. Zhou et al., 2007) as well as in unaffected siblings (H. Liu et al., 2012) and individuals at ultra-high risk for psychosis (Shim et al., 2010), supporting claims that aberrant DMN function may serve as an endophenotype of the disorder. Hyperconnectivity of DMN in SZ and first-degree relatives has also been observed during a working memory task (Whitfield-Gabrieli et al., 2009). SZ and their first-degree relatives demonstrated less task-related suppression of DMN than did HC. Importantly, task-related DMN suppression predicted performance such that greater DMN suppression was associated with better working memory performance. Similar findings were obtained in a study in which patients with recent-onset schizophrenia (within 5 years of initial treatment for psychosis) as well as ultra-high-risk individuals demonstrated deficient DMN suppression during a test of working memory (Fryer et al., 2013). Although the majority of studies have found DMN functional hyperconnectivity in SZ, findings from studies using a first-episode (FE) sample have been mixed, as discussed below under Study Aim 1.

Evaluation of Default Mode Network Using EEG

To our knowledge, very few studies have specifically evaluated DMN function in SZ using EEG oscillatory analysis. Unlike ERP components, which capture brief neural responses on the order of milliseconds to discrete stimuli, neural oscillations are rhythmic patterns of neural activity that can be examined on the order of seconds (Bell & Cuevas, 2012). Synchronization, or coupling, of the oscillatory activity measured by scalp electrodes or inferred about brain sources

may reflect communication between brain regions, thus providing a measure of network connectivity (Bakhshayesh et al., 2019).

Previous studies using EEG to make claims about schizophrenia-associated alterations in DMN function have generally not computed functional connectivity using EEG data (e.g., coherence, synchrony, etc.), but instead have linked non-source-localized EEG frequency-band power to fMRI-assessed DMN connectivity (Baenninger et al., 2017; Wang et al., 2017; Won et al., 2018). In a recent study examining resting state coupling of DMN-related regions using EEG oscillatory data, Lee et al. (2019) found support for DMN hyperactivation in FE SZ. To our knowledge, this is the only published study of DMN connectivity in SZ assessed using EEG oscillatory data in SZ.

Employing EEG in the investigation of network activity has the potential to improve upon traditional analyses using fMRI data by providing quantification of changes in neural activity that cannot be fully understood when using only fMRI due, for example, to rapid time course (e.g., Popov et al., 2018b). Evidence suggests that functional connectivity varies considerably over time, such that the coupling observed between spatially disparate brain regions is associated with temporally variable neuronal dynamics (Chang & Glover, 2010). EEG may be particularly well-suited to investigations of neural networks due to its ability to capture synchronization of neural activity at the millisecond level, providing a measure of the extent of functional connectivity within large-scale networks moment-to-moment. Notably, EEG provides the temporal resolution necessary to capture fast neuronal changes of interest during research tasks such as the paired-stimulus paradigm.

Given its sensitivity to temporal dynamics, EEG also has the ability to clarify the structure and function of networks defined with fMRI. For example, given the limited temporal resolution

of fMRI, networks defined using hemodynamic imaging may actually result from the time average of multiple, transiently synchronized sub-networks (e.g. spatial inhomogeneity; Brookes et al., 2014), each of which may demonstrate its own spatial signature and implement different cognitive processes. Additionally, assessment of neural networks with EEG fosters examination of connectivity that may depend on a specific frequency band of neural oscillations, such that neural networks are organized by neuronal activity at distinct frequencies, with implications for specific disorder-related pathology and associated roles in cognitive function and symptom presentation (Newson & Thiagarajan, 2019). Although spatial resolution has often been cited as a drawback in the use of EEG in studying networks in which spatially distributed brain regions are simultaneously active, advances in source localization techniques improve the ability to deduce the underlying neural sources associated with scalp activity (Michel & He, 2019). That said, fMRI still typically provides better spatial resolution for brain mapping for slower phenomenon, especially if deep brain regions of interest include those whose location may be difficult to infer from neuronal activity measured on the scalp (e.g., amygdala; Liu, Farahibozorg, Porcaro, Wenderoth, & Mantini, 2017). Thus, employing both fMRI and EEG in assessment of neural network function capitalizes on the relative strengths of both modalities and may provide the best means for elucidating the spatial maps and time courses of network function and dynamics not available from one modality alone. Multimodal analysis additionally provides better specificity for mapping neural network function to specific cognitive deficits and clinical symptoms. Accordingly, combined fMRI and EEG analysis was undertaken for the present project to advance the assessment of DMN function in schizophrenia.

Salience Network

In contrast to DMN, SAL is considered a higher-order system supporting determination of the proximal salience of stimuli, initiating appropriate cognitive control, and performing context-specific stimulus selection necessary for enhancing access to cognitive resources needed for goal-directed behavior, such as the activation of executive networks (Menon, 2015; Menon & Uddin, 2010). Unlike typically fast, automatic, "bottom-up" notions of salience detection, SAL is implicated in higher-order filtering and amplification of stimuli (Menon & Uddin, 2010). One theory posits that SAL serves as a "cortical out-flow hub" responsible for coordinating changes in activity across multiple brain networks (Bonnelle et al., 2012; Ham et al., 2013; Sridharan et al., 2008). Specifically, results of studies suggest a causal role for SAL in initiating switching between DMN and central executive network (CEN; see Figure 1) (Menon, 2011). In line with that view of normal SAL function, abnormal intra- and inter-network SAL connectivity in SZ has been proposed as a mechanism associated with aberrant attribution of salience to stimuli and dysfunctional switching between externally-directed and internally-directed cognitive processes (O'Neill et al., 2019).

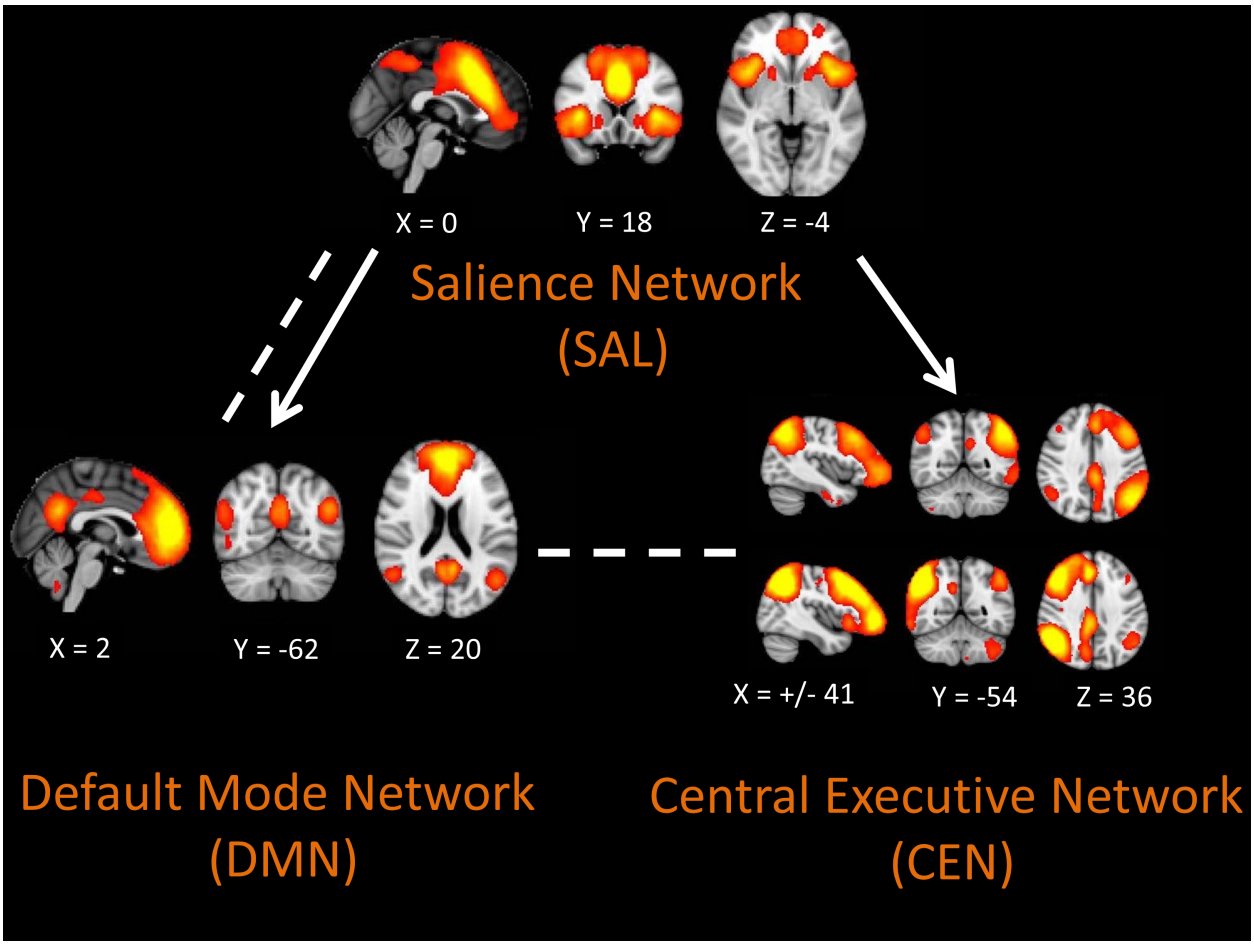

Figure 1: Conceptual diagram demonstrating hierarchical organization of default (DMN), salience (SAL), and central executive (CEN) networks in healthy individuals. Arrows denote proposed causal or modulatory relationships. Dashed lines denote negative correlation between networks. Brain images are from a previously published set of templates from the BrainMap Database (Laird et al., 2005).

Network Disruptions in Schizophrenia

In HC, activity in SAL and CEN increases during cognitive tasks that require attention to external stimuli (Dosenbach et al., 2007), whereas DMN activity is suppressed (Greicius et al., 2003; Raichle, 2015). Although interactions between the three core networks are critical for cognitive processing, the relationship between DMN and SAL is particularly relevant to tasks requiring the switching of attention between externally- and internally-generated stimuli and may be key to understanding mechanisms of interest in SZ (Menon & Uddin, 2010; Putcha et al., 2016). One recent fMRI study of FE SZ found increased connectivity between DMN and SAL

hubs (i.e., the central and highly connected nodes within networks) when patients reported experiencing auditory hallucinations (Mallikarjun et al., 2018). Another study found that intra-network DMN and lagged inter-network DMN-SAL connectivity were associated with positive symptoms, such as thought disorder, as well as negative symptoms, including attentional deficits (Hare et al., 2019). Thus, temporal dynamics and communication between DMN and SAL represent promising areas of research for elucidating the mechanisms associated with cognitive impairments and clinical symptoms of SZ.

Given the role of DMN in internally-driven processing, successful down-regulation of DMN may be part of a mechanism supporting filtering of unnecessary information via disengagement from distracting or irrelevant information. Consistent with a hierarchical model wherein SAL plays a causal role in switching between DMN and CEN, abnormal SAL function -- specifically a failure of DMN down-regulation by SAL -- may drive aberrant DMN connectivity and associated deficits, including impaired attention allocation to relevant stimuli and prolonged processing of irrelevant stimuli. These attentional allocation and inhibitory filtering processes can be indexed by N100 amplitude to S1 and by N100 suppression, respectively, during the paired stimulus paradigm. Additionally, prior work has shown that among the neural generators of N100 are regions of DMN and SAL, including parietal and cingulate cortices (Boutros et al., 2010).

Project Overview

The overarching goal of the present dissertation was to determine how disruptions to communication processes within and between DMN and SAL are associated with dysfunction in SZ. This was accomplished via three specific aims, outlined below. A multimodal approach was

employed, using EEG and fMRI, to characterize mechanisms of abnormal salience and inhibitory processing in SZ that may play a role in vulnerability to and maintenance of disorder-related impairments and targets for such interventions as cognitive training, antipsychotic medication, and transcranial direct current stimulation. In the present study, it was hypothesized that these neural network measures and the N100 variables under investigation capture disorder-related dysfunction in shared mechanisms of salience and inhibitory processing and would thus be related**.** Specifically, different intra- and inter-network properties of DMN and SAL may correspond to distinct aspects of processing during the paired stimulus paradigm, such that the function of one neural circuit predicts voluntary attention allocation reflected in N100 amplitude to S1, whereas another circuit is associated with impairments in N100 suppression as measured by the ratio score. Although relationships with measures of positive and negative clinical symptoms were not within the scope of the present study, follow-up analyses are planned and will serve to clarify the roles of DMN and SAL dysfunction in the disorder.

The broad term "connectivity" is often used to describe functional or statistical relationships between physiological phenomena over time. In the present dissertation, the specific method used for quantifying network connectivity using oscillatory EEG data was coherence (see method for Aim 1). No such specific label is used to distinguish connectivity assessed with fMRI in the literature, therefore "connectivity" can refer to general network connectivity assessed with any method, or can refer specifically to fMRI assessments of connectivity. Throughout the present study, modality-specific terminology is used to clarify which modality provided a particular estimate of connectivity (oscillatory EEG data using coherence or fMRI data), or if instead the term refers to the concept of network connectivity more broadly.

This dissertation expanded upon a currently-funded NIMH R01 randomized controlled trial (RCT; PI: Nuechterlein) and its funded Competitive Revision (MPIs: Yee-Bradbury, Miller, Nuechterlein). Data for the dissertation were obtained from participants with SZ prior to intervention under the RCT. At pre-treatment baseline, EEG was recorded during a paired-stimulus paradigm, rs-fMRI was obtained, and measures of cognitive targets and clinical symptoms were administered. Demographically-matched HC, who did not undergo any intervention, completed all but the symptom measures. The research questions and analyses addressed by the dissertation are unique to this project and do not overlap with either of the R01s.

Study Aim 1: Clarify the default state in SZ via multimodal replication of resting state DMN hyperconnectivity in FE SZ

Increased connectivity within DMN may contribute to psychotic symptoms (e.g., paranoia, thought disorder, and hallucinations; Rotarska-Jagiela et al., 2010) as well as cognitive deficits, such that DMN-associated goal-irrelevant functions interfere with goal-directed cognitive processes (Anticevic et al., 2012). Although the majority of previous work suggests a pattern of DMN hyperconnectivity in SZ at rest, findings are mixed in FE SZ. Contrary to reports of disorder-related hyperconnectivity, two recent fMRI studies reported that individuals with FE SZ exhibited hypoconnectivity in DMN (Fan et al., 2019; O'Neill et al., 2019). One interpretation of these conflicting findings is that observations of DMN hyperconnectivity, most reliably in chronic SZ, are the result of compensatory mechanisms that develop over the course of the disorder in response to generalized functional dysconnectivity of large-scale networks in early psychosis (O'Neill et al., 2019). As such, intrinsic DMN hyperconnectivity is posited to occur

after illness onset and to represent a core pathological change during the course of SZ rather than a stable endophenotype of the disorder.

In order to address the mechanistic function of aberrant DMN connectivity as a potential endophenotype of SZ, Study Aim 1 sought to clarify the nature of aberrant connectivity within DMN at rest in FE SZ. In order to determine whether DMN hyperconnectivity is a stable, state-independent, and reliable neural marker of SZ, replication specifically with a FE population could provide further evidence for DMN hyperconnectivity either as a vulnerability marker for the development of SZ that could be used for early diagnosis, or instead as a neural phenomenon that arises over the course of illness that could represent a valuable target for preventive treatment. Thus, the present study investigated whether FE SZ demonstrate intra-DMN hyperconnectivity at rest, as observed previously using EEG in FE SZ (Lee et al., 2019) and using fMRI in chronic SZ (e.g., Garrity et al., 2007; Jafri et al., 2008), or instead whether a dissociation exists between the two modalities in observed intra-DMN connectivity in FE SZ, with fMRI revealing hypoconnectivity (e.g., Fan et al., 2019; O'Neill et al., 2019).

Method

Participants

Data from a total of 52 SZ and 25 HC were available for the dissertation project although EEG and fMRI were not collected from all participants. For Study Aim 1, resting state EEG was available for 26 SZ and 25 HC while fMRI data were obtained from 38 SZ and 20 HC. All patients met DSM-5 criteria for SZ, schizophreniform disorder, or schizoaffective disorder depressed type, and were enrolled in the RCT through the UCLA Aftercare Research Program. HC were recruited from the greater Los Angeles community and were demographically matched

to the patient sample on age, gender, race/ethnicity, and parental education. Opportunities to participate in the study were advertised via flyers placed at local universities, businesses, and community centers, as well as advertisements placed on the internet. Prospective participants were screened via phone for initial eligibility requirements and then underwent a structured clinical interview for the DSM-5 (SCID) to evaluate eligibility.

Inclusion and exclusion criteria for patient participants included: a first episode of a psychotic illness that began within the past two years; between 18 and 45 years of age; no evidence of a known neurological disorder (e.g., epilepsy) or significant head injury; no evidence of alcohol or substance use disorder within the six months prior to the first episode and no evidence that substance abuse triggered the psychotic episode or made the schizophrenia diagnosis ambiguous; and no mental retardation (i.e., premorbid IQ not less than 70).

Inclusion and exclusion criteria for HC were as follows: no history of any DSM-5 schizophrenia-spectrum or other psychotic disorder; no current or recurrent major depressive disorder; no past major depressive episode that lasted longer than one year; no history of bipolar disorder, obsessive-compulsive disorder, post-traumatic stress disorder, neurological disorder or other physical disorder (e.g., significant head injury) that could affect brain functioning; no history of alcohol/substance use disorder; and no family history of any psychotic disorder among first-degree relatives. All participants were required to exhibit sufficient acculturation and fluency in the English language to avoid invalidating research measures and were excluded if currently pregnant or lactating.

Measures

EEG Procedures.

EEG data were obtained while participants were seated comfortably in a sound-isolated, climate-controlled chamber with audio and visual monitoring. EEG was recorded on a Brain Products system from 96 scalp locations using actiCAP active electrodes referenced to the left mastoid and later re-referenced to average mastoids (Miller, Lutzenberger, & Elbert, 1991). At collection, sampling rate of EEG and EOG data was 2000 Hz and used a bandpass of 0.05 to 200 Hz. Electrodes were placed above, below, and near the canthus of each eye to record horizontal and vertical EOG, which was recorded for removal of blink and saccade artifact. All impedances were below 25kΩ. Participants underwent 5 minutes of resting-state EEG during which they were instructed to remain awake and keep their eyes focused on a neutral fixation cross. Vertical and horizontal EOG were included in the recording montage for artifact removal and high-quality source modeling. A CapTrak spatial digitizer provided 3D coordinates of the electrode positions, and fiducial landmarks were co-registered with each participant's high-resolution structural MRI. Scalp-space ERP, source-space oscillatory, and connectivity analyses were conducted with FieldTrip, BESA Research, and scripts written in MATLAB. Pre-processing of EEG included visual inspection of data. For each participant, 20 seconds of data exhibiting eye movement, including blinks and saccades, were specified with at least 3-5 blinks within this selected data when possible. Independent Component Analysis (ICA) using the Extended Infomax algorithm was conducted to identify eye and other artifact (e.g., heart rate/EKG, channel noise, line noise, muscle) components. Data were reconstructed excluding artifact components and then underwent further artifact rejection using the artifact scanning tool of BESA.

MRI Procedures.

MRI was done on a 3T Siemens Prisma at the UCLA Staglin Center for Cognitive Neuroscience. Participant head movement was minimized with foam padding. At each session, a high-resolution, T1-weighted, anatomical scan was acquired using an MPRAGE sequence with 208 interleaved slices (TR = 2500 ms; TE 2.14 ms; slice thickness = 0.8 mm; flip angle = 8 degrees). Resting-state BOLD data were acquired using a 6.5-minute sequence with 72 interleaved slices (TR = 800 ms; TE = 37 ms; flip angle = 52 degrees). During rs-fMRI data collection, participants were instructed to remain awake and keep their eyes focused on a neutral fixation cross. rs-fMRI data were collected approximately 35 minutes after the start of scanning, allowing time for acclimation to scanning conditions. The first four volumes, non-steady state or dummy scans, were discarded as part of the scanner sequence.

Pre-processing of structural and rs-fMRI data was performed using the FMRIB Software Library suite (FSL; http://fsl.fmrib.ox.ac.uk/fsl/fslwiki/) and the Graph Theory GLM (GTG) MATLAB toolbox (www.nitrc.org/projects/metalab_gtg) with structural brain extraction using The Advanced Normalizations Tools ecosystem, or ANTs (Tustison et al., 2021). In brief, fieldmap images were bias-corrected, brain-extracted, and eroded to ensure that noisy boundary voxels were excluded. Bias-correction and brain-extraction were performed on T1 images. Images were corrected for motion using rigid-body transformations via MCFLIRT and registered to MNI space. Spatial smoothing was not employed as it could impact accurate identification of the a priori ROIs and spatial noise is already decreased by the use of spherical ROIs in which average signal is computed across voxels within the ROI. FSL ICA-AROMA was used to identify and remove noise and motion components (Pruim et al., 2015). DVARS (spatial root mean square of data after temporal differencing, i.e. amount of BOLD intensity change across the entire brain from the previous timepoint) was calculated and used to eliminate individuals

with excessive motion throughout the scan (Power et al., 2014). Briefly, individuals with more than 5 volumes with DVARS = 0.5 were flagged for visual inspection of the timeseries for remaining visible motion artifacts. If no gross motion problems were observed during this visual inspection, the data were included. If motion artifacts were still evident in the timeseries, spike regression was performed. Masks for white matter and cerebrospinal fluid were used to extract the average time course for these sources of physiological noise from each participant. The resulting time courses were included as nuisance regressors during first-level analyses.

Definition of Neural Networks

DMN and SAL networks were defined using a priori regions and coordinates were drawn from seminal published works in the MRI literature (Power et al., 2011; Sridharan et al., 2008; Table 1). The same regions and corresponding coordinates were used to define both regional sources in the EEG data and the ROIs employed in fMRI analyses. Spherical ROIs were used in all fMRI analyses (Figure 1). The size of spherical ROIs was intended to maximize inclusion of voxels in the relevant brain regions while minimizing white-matter and cerebrospinal fluid inclusion. To this end, midline regions (PCC, PFC, ACC) were split into two lateralized (left and right) spherical ROIs in order to maximize regional gray matter inclusion while reducing midline CSF inclusion.

Table 1. The network, name, and location (in MNI space) of regions used for network connectivity analyses.

Network	Region	Central Coordinates (MNI)			Diameter of fMRI ROI(s) (mm)	Offset for Lateralized ROIs (X; MNI)
		X	Y	Z		
DMN	Posterior Cingulate Cortex (PCC)	1	-51	29	4	+7; -5
DMN	Prefrontal Cortex (PFC)	-1	61	22	2	+/- 5
DMN	Left Angular Gyrus (lAG)	-48	-66	34	4	
DMN	Right Angular Gyrus (rAG)	53	-61	35	4	
DMN	Left Lateral Temporal Cortex (lLat)	-65	-23	-9	4	
DMN	Right Lateral Temporal Cortex (rLat)	61	-21	-12	4	
SAL	Right Frontal Insular Cortex (rFIC)	37	25	-4	4	
SAL	Left Frontal Insular Cortex (lFIC)	-32	24	-6	4	
SAL	Anterior Cingulate Cortex (ACC)	4	30	30	4	+2; -10

Note: Central coordinates for DMN come from Power et al. (2011) and central coordinates for SAL come from Sridharan et al. (2008). For spherical ROIs created for fMRI analyses, also included is the offset (from central coordinate) used for midline regions for which separate left and right ROIs were created to reduce inclusion of midline cerebrospinal fluid (non-brain). The diameter of the fMRI spherical ROIs created is also included (in mm).

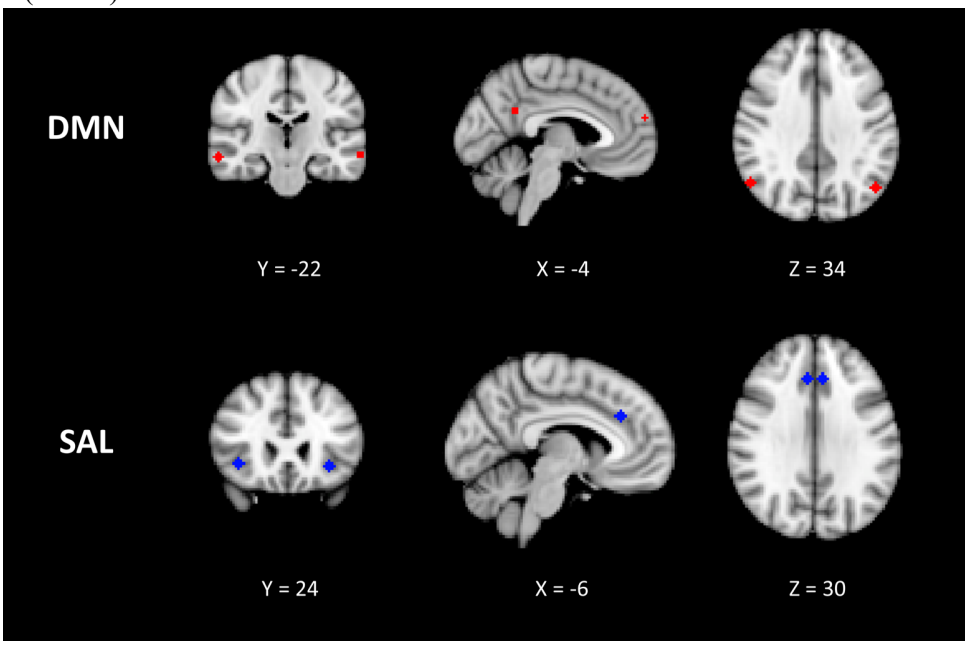

Figure 2. Spherical regions of analysis created for functional and effective connectivity analyses with fMRI data. A) Default mode network (DMN) defined in the present study using regions from Power et al.,

2011. B) Salience network defined in the present study using regions from Sridharan et al., 2008. Region names, central coordinates, and the size of spherical regions used for fMRI analyses are provided in Table 1.

fMRI-derived DMN Analyses

Intra-network functional connectivity matrices for DMN using the nodes identified by Power and colleagues (2011) were calculated for each participant by using the GTG toolbox to compute pairwise robust correlation coefficients between the average time series of the identified nodes. Processing included temporal high-pass filtering (0.01 Hz) using a Butterworth filter, second-order temporal detrending, and partialling of each participant's mean global signal and mean white matter and ventricular signals. Time-series data were extracted from each DMN ROI as the largest principal component across voxels in an ROI for each time point. ROIs were excluded from time-series extraction if the segmentation included fewer than 5 voxels or less than 25% of the voxels within the ROI. All participants retained complete time series data for all 6 DMN ROIs and therefore were available for analysis. A composite score for each participant was computed by averaging robust correlation coefficients within the DMN (Guha et al., 2016). SZ and HC intra-network DMN connectivity was compared using independent samples t-tests.

EEG-derived DMN Analyses

In order to assess DMN using EEG data, source localization using CapTrak data enabled the generation of regional sources at the same DMN ROIs used in the rs-fMRI analysis (Power et al., 2011; Figure 3). Frequency-resolved coherence was used to test a spectrum of potential frequencies (2-40 Hz). Complex demodulation was used for time-frequency analyses with a time-frequency sampling of 1 Hz, 50 ms. A 50 Hz lowpass filter was applied during the time-frequency analysis (Popov et al., 2018a).

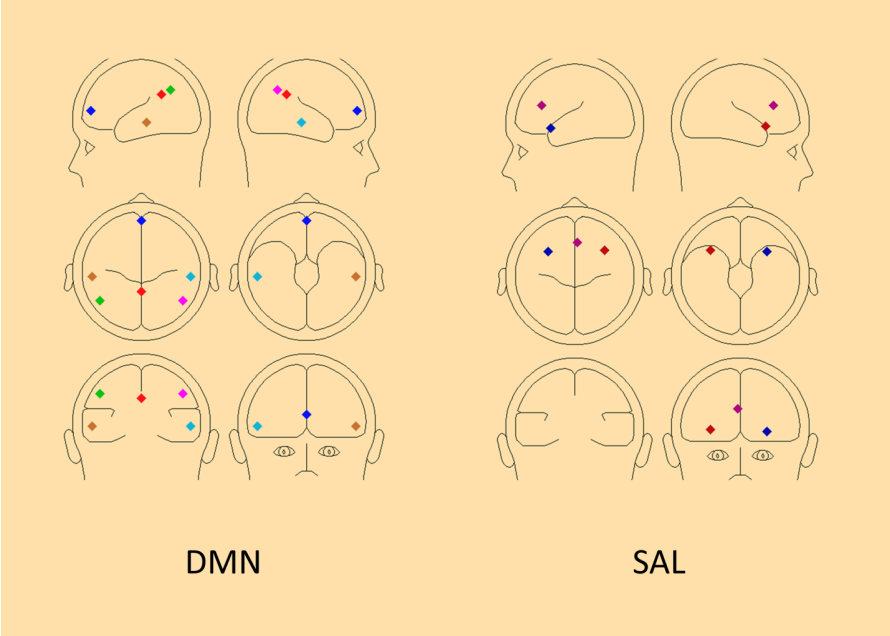

Figure 3. Regional sources used for oscillatory connectivity analyses with EEG data. Left: Default mode network (DMN) defined in the present study using regions from Power et al., 2011. Right: Salience network defined in the present study using regions from Sridharan et al., 2008. Region names, central coordinates, and the size of spherical regions used for fMRI analyses are provided in Table 1.

Imaginary coherence was computed between nodes of DMN, with higher coherence corresponding to stronger intra-network connectivity (Nolte et al., 2004), as the imaginary component of oscillatory activity avoids problems with volume conduction. Group differences (SZ, HC) were assessed using cluster-based permutation testing. Monte Carlo randomization using 5000 randomizations was used to identify clusters (in latency and frequency) exhibiting group differences that exceeded a 5% significance threshold.

Results

Participant Data

Demographic and clinical characteristics of all study participants are presented in Table 2. There were no significant differences between SZ and HC on any of the demographic

measures for the entire sample or for the subset of participants included in the analyses associated with Study Aim 1.

Table 2. Demographic and clinical characteristics for the entire sample of schizophrenia and healthy comparison participants included in the dissertation project.

	SZ (N = 52)	HC (N = 25)
Age (average in years)	21.6 (3.5)	20.2 (2.2)
Gender (% female)	25%	36%
Education (avg. years)	13.7 (1.7)	13.7 (1.4)
Parent Education	14.9 (3.5)	14.9 (3.7)
Race/Ethnicity		
White	69%	60%
Black	10%	4%
Asian	15%	28%
Other/Unknown	8%	8%
Hispanic	35%	40%
Diagnosis Schizophrenia Schizoaffective Schizophreniform	 79% 3% 17%	
Antipsychotic Dosage (mg/day, CPZ equiv.)	156.4 (213.3)	

rs-EEG-derived DMN Coherence

Consistent with prior reports, SZ demonstrated greater resting state intra-DMN hyperconnectivity compared to HC as exhibited by greater coherence in the 25-30 Hz (beta) range (Figure 4a). However, the group difference did not survive clustering with permutation

testing. To assess the magnitude of difference in intra-DMN connectivity between SZ and HC in this frequency band, average coherence was extracted from this "cluster" for each participant. Within this "cluster," the size of the effect was moderately large *(t(50)=2.33, p = 0.02, d = 0.7;* Figure 4b), suggesting that the lack of significant clustering may have been due to insufficient power related to sample size.

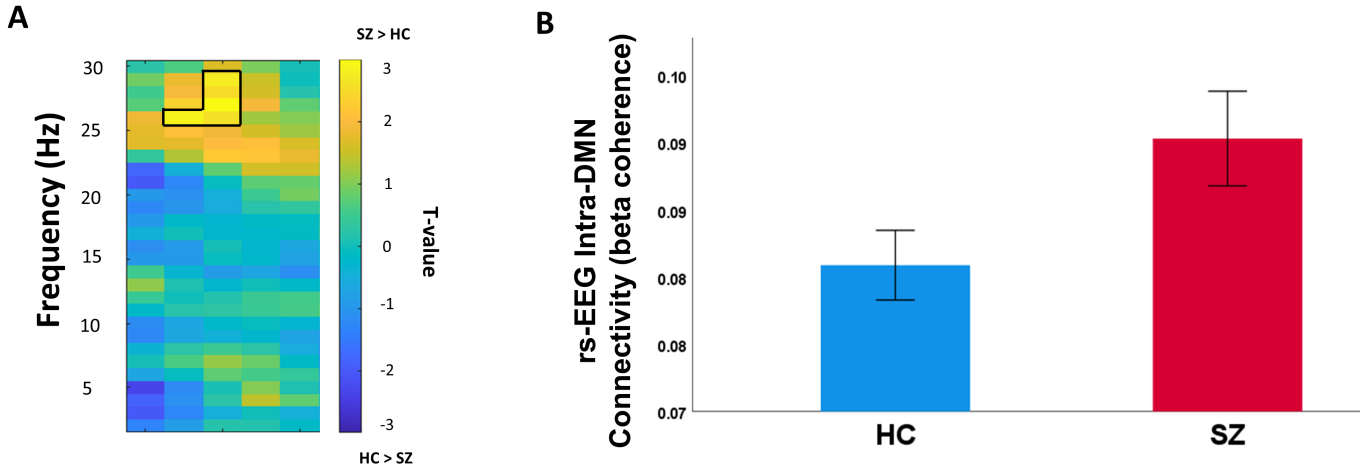

Figure 4. Group (SZ, HC) differences in intra-DMN coherence at rest. A) Yellow (positive t-values) "cluster" between 25-30 Hz, outlined in black, denotes greater coherence in SZ than HC. Time in seconds is shown on the x-axis, and frequency is shown on the y-axis. An epoch of 2.25 seconds is displayed. B) Extracted average coherence within the highlighted 25-30 Hz beta-band "cluster" for SZ (red) and HC (blue). Error bars denote +/- SE.

rs-fMRI-Derived DMN Connectivity

Data from one participant in the SZ group was identified as a statistical outlier (> 3 SD from group mean) and excluded from analyses of rs-fMRI-derived DMN connectivity. In

evaluating group differences using rs-fMRI, SZ demonstrated a statistical trend for higher intra-DMN connectivity (*M = 0.3, SD = 0.2*) than HC (*M = 0.2, SD = 0.08*; *t(65)=1.6, p = .1, d= 0.4;* Figure 5*).*

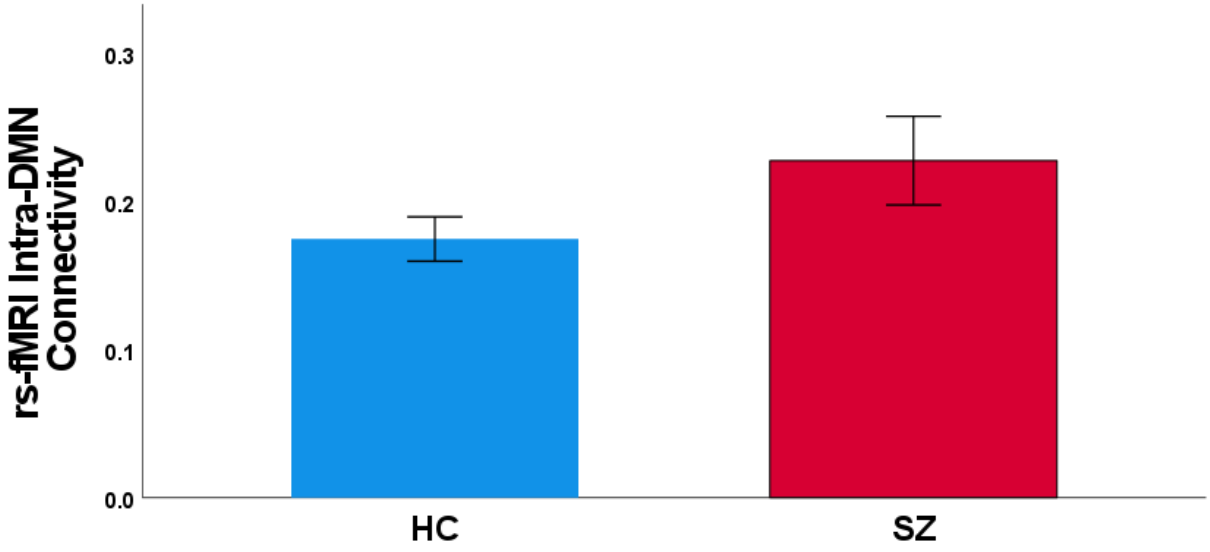

Figure 5. Group (SZ, HC) differences in intra-DMN connectivity at rest. SZ (red) demonstrate higher intra-DMN connectivity than HC (blue). Error bars denote +/- SE.

Multimodal Data Fusion: Relationships Between rs-EEG- and rs-fMRI-derived Intra-DMN Coherence

To examine relationships between intra-DMN connectivity across modalities, simple correlations between connectivity assessed with beta rs-EEG oscillatory coherence and with rs-fMRI were computed across all participants. Results demonstrated a positive relationship (*r(31) = 0.4, p = 0.04*), such that higher intra-DMN beta coherence was associated with higher intra-DMN fMRI connectivity. To assess possible differences in this relationship between SZ and HC, a regression analysis examined Group status and rs-fMRI-derived intra-DMN connectivity as

predictors of rs-EEG-derived intra-DMN connectivity. Group *(β = 0.4, t(28) = 2.2, p=0.02*) and rs-fMRI-derived intra-DMN connectivity *(β = 0.4, t(28) = 2.3, p=0.03*) each contributed unique variance (Figure 6). The groups showed *(*no interaction; *β = 0.3, t(27) = 0.7, p=0.6*).

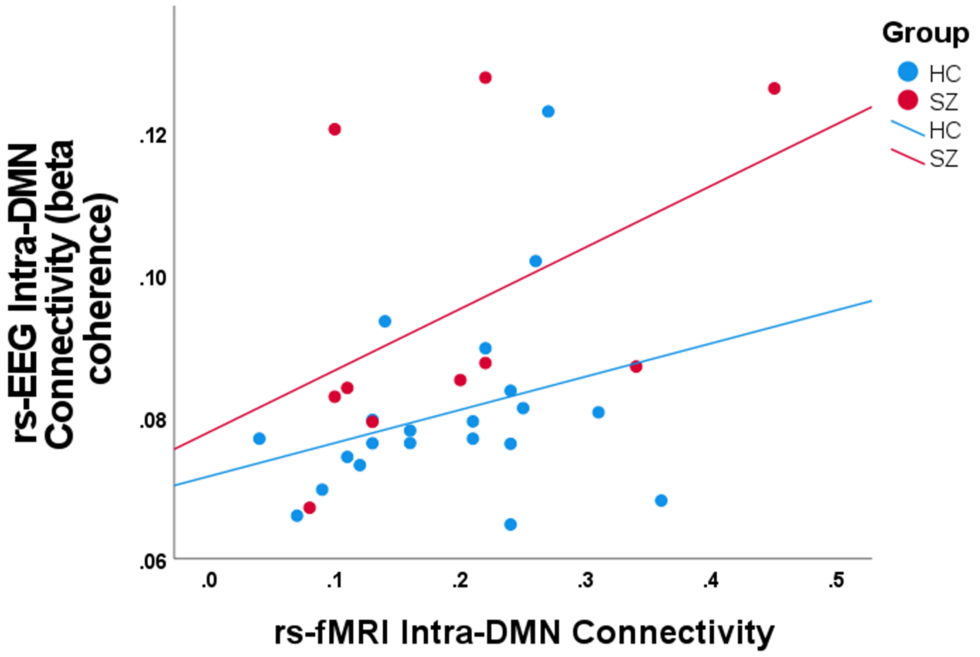

Figure 6. Both SZ (red) and HC (blue) demonstrate a positive relationship between rs-fMRI-derived intra-DMN connectivity, on the x-axis, and rs-EEG-derived intra-DMN connectivity (beta coherence), on the y-axis.

Discussion

The present FE SZ sample provided evidence of resting state DMN hyperconnectivity in both EEG and fMRI, although the statistical support from these two-tailed tests was marginal for both measures. A strong case for one-tailed tests would not be supported by the small and

inconsistent FE SZ literature, but the observed effect sizes were substantial for both measures. Present data provide some internal replication, given the same direction of effect in two different measures of DMN connectivity assessed during different visits, and the moderate correlation between the two measures ($r = 0.4$). Reliance on the larger SZ literature not limited to FE samples would provide some justification for one-tailed tests, and both rs-EEG and rs-fMRI connectivity, even though assessed in separate visits, met that statistical threshold. Interpreting the present pattern of findings as replicating DMN hyperconnectivity in SZ (Hu et al, 2017; Lin et al., 2012; Zhou et al., 2007; Shim et al., 2010; Galindo et al., 2018), present results indicate that DMN hyperconnectivity can be observed in SZ during the first episode of illness.

One theory posits that resting state DMN hyperconnectivity reflects a compensatory mechanism that develops over the course of illness as a response to generalized functional dysconnectivity (O'Neill et al., 2019). However, present evidence of hyperconnectivity in a FE SZ sample is consistent with the alternative view that this is a core process associated with the disorder rather than a later, secondary effect of the disease (Liu et al., 2012; Whitfield-Gabrieli et al., 2009). This finding suggests that hyperconnectivity of the DMN is a reliable feature of disorder-related dysfunction.

Although present findings of resting state DMN hyperconnectivity in SZ are consistent with several previous studies (see review by Hu et al., 2017), findings using FE samples have been mixed with some studies demonstrating hypoconnectivity of DMN in this population. Discrepancy in the nature of DMN abnormalities in SZ across studies may relate to methodological differences. Fan and colleagues (2019) reported resting state DMN hypoconnectivity, with resting state fMRI collected while FE SZ were instructed to close their eyes. In the meta-analysis by O'Neill and colleagues (2019), 8 of the 11 studies collected resting

state data with eyes closed (EC) while the remaining three studies did not report this information. Although connectivity within DMN has largely been found to be consistent across resting conditions [EC, eyes open (EO), eyes open with fixation (EO+F)], EC has been found to produce less connectivity within DMN than assessment with EO+F (Yan et al., 2009; Van Dijk et al., 2010). Assessment of resting state DMN connectivity with EO+F has been identified to be more reliable than either EO or EC (Patriat et al., 2013); the present study relied on this approach. Differences in functional connectivity could relate to the increase in non-goal-directed visual information processing during EO relative to EC, which may contribute to an increase in mind-wandering and daydreaming, thus bolstering DMN activity (Yan et al., 2009).

Differences between EO and EC conditions may also relate to differences in alpha oscillations, which are greater in EC vs. EO conditions (Berger, 1929, 1930). Alpha power has been found to be negatively related to fMRI fluctuations in DMN regions (Bowman et al., 2017), thus increased alpha during EC resting state conditions may impede reliable assessment of DMN. The present substantial and statistically reliable correlation between rs-EEG and rs-fMRI intra-DMN connectivity provides converging evidence that EC+F is an appropriate context for characterizing resting state DMN connectivity.

By demonstrating DMN hyperconnectivity, results from the present FE sample augment work in chronic SZ (e.g., Garrity et al., 2007; Jafri et al., 2008), unaffected siblings (H. Liu et al., 2012), and individuals at ultra-high risk for psychosis (Shim et al., 2010). The mechanism through which DMN hyperconnectivity may confer risk for psychosis is not yet clearly understood. DMN is hypothesized to support self-referential processing, which encompasses the ability to distinguish stimuli related to one's self from those that may be externally generated (Buckner et al., 2008; Northoff et al., 2006). Self-disturbance, a fragmented understanding of the

self that is associated with the inability to see one's self as the originator of internal experiences (e.g., thoughts and feelings) is classically considered to be at the core of schizophrenia (Nelson et al., 2014c). Identifying mechanisms that support self-referential processing, dysfunction of which may predispose individuals to self-disturbance, may be especially important for understanding the pathology and treatment of the disorder. Accordingly, DMN hyperconnectivity may confer risk for the development of SZ via alterations in self-referential processing, as evidenced by research finding that these intrinsic alterations in DMN are observed even among individuals at increased genetic risk for developing SZ (van Buuren et al., 2012). Increased connectivity of DMN at rest may also provide a potential mechanism supporting such aberrant processes as abnormal inner-directed rumination that may increase susceptibility to self-disturbance and related psychotic symptoms.

This study analyzed resting state connectivity of DMN using EEG oscillatory data, allowing for examination of connectivity that may be dependent on the frequency band of neural oscillations. Present findings pointed to DMN hyperconnectivity among SZ within the beta frequency band. Several studies with HC have demonstrated relationships between beta-band EEG activity and DMN function, though typically the approach has involved correlating non-source-localized EEG frequency-band power and fMRI-derived connectivity of DMN (e.g., Hlinka et al., 2010; Laufs et al., 2003; Neuner et al., 2014). Researchers have suggested that beta activity modulates maintenance of the "status quo" for cognition (Engel et al., 2010) related to the proposed functions of the DMN. Present findings build on such a view by demonstrating that not just beta power, but explicit beta connectivity of DMN as assessed via coherence, correlates with rs-fMRI-derived intra-DMN connectivity and that alterations in this connectivity are observed in FE SZ .

The 0.4 correlation between DMN connectivity assessed with rs-EEG beta coherence and assessed with rs-fMRI indicates a nontrivial relationship but with other sources of variance contributing substantially as well. One explanation for observed discrepancies between EEG-derived and fMRI-derived network connectivity pertains to differences in their temporal resolutions. Because functional connectivity can vary considerably over time (Chang & Glover, 2010), EEG may have captured systematic changes in network connectivity that fMRI missed. In the present study, EEG captured DMN connectivity associated with neural network activity in the beta frequency band (25-30 Hz) whereas fMRI captured much slower DMN connectivity (0.01–0.25 Hz; Gohel & Biswal, 2015). It is likely that different cognitive functions are subserved by frequency-specific neural oscillations, such that the connectivity indexed by beta (EEG) vs. much slower (fMRI) frequencies relates to distinct cognitive processes. This was further explored by examining their relationships with N100 measures in Study Aim 2.

In summary, FE SZ patients in the present study provided some evidence of resting state hyperconnectivity within DMN as assessed with both EEG oscillatory and fMRI data, obtained during separate study visits. Group differences in EEG-assessed DMN connectivity were specifically found in the beta frequency band. Furthermore, EEG-assessed DMN beta coherence and fMRI-assessed DMN connectivity were positively related, demonstrating DMN hyperconnectivity in SZ even across imaging modalities, although the measures also likely capture distinct aspects of DMN activity. To further elucidate the impact of DMN dysfunction on cognition in SZ, pursuit of Study Aim 2 built upon these findings by examining how intra-DMN connectivity relates to measures of attention and inhibitory processing as assessed via the N100 ERP component.

Study Aim 2: Evaluate differences in DMN suppression between FE SZ and HC, and determine whether DMN suppression represents a mechanism supporting salience and inhibitory processing

Functionally, suppression of DMN may reflect disengagement from distracting cognitive processing in order to effectively filter redundant or unnecessary information that is either externally- or internally-generated (Anticevic et al., 2012; Chadick & Gazzaley, 2011). DMN suppression may be a mechanism through which interference by goal-irrelevant functions associated with the DMN, such as self-referential processing and daydreaming, is reduced. Observations of DMN hyperconnectivity in SZ may correspond to insufficient suppression of DMN, resulting in more internally-oriented cognitive processing that could limit allocation of attention to relevant stimuli as well as limiting suppression of irrelevant stimulus processing (Anticevic et al., 2012). Therefore, it was hypothesized that DMN suppression would be associated with attention processes indexed by N100. Specifically, SZ were expected to exhibit less suppression of DMN than HC during the paired stimulus paradigm and at rest, which in turn would predict lower S1 N100 amplitude and higher N100 ratio scores.

It is unclear whether SZ demonstrate a different relationship between DMN suppression and cognitive functioning than HC or whether SZ demonstrate less DMN suppression, which in turn predicts and perhaps fosters cognitive dysfunction. The first of these possibilities suggests an interaction between patient status and DMN suppression, whereas the second suggests a set of relationships wherein the effect of patient status on cognitive dysfunction is mediated by less successful DMN suppression. Because it is unclear whether the moderation hypothesis or the mediation hypothesis holds, both moderation and exploratory mediation analyses were included to achieve Study Aim 2.

Due to the present goal of elucidating neural network dynamics during the course of the paired stimulus paradigm, evaluation of these networks employed connectivity analyses using EEG oscillatory data. EEG is an ideal modality at the time scale of DMN suppression from pre- to post-auditory stimulus, whereas the temporal resolution of fMRI is not sensitive enough to capture this phenomenon.

To complement analysis of EEG-derived DMN suppression during the paired stimulus paradigm, resting state EEG and fMRI data were also employed to investigate intrinsic resting state DMN function. EEG-assessed DMN suppression during the paired stimulus paradigm was used to capture the temporal evolution of network activity during attentional and inhibitory processing related to the task, whereas resting state-assessed DMN intra-network activity was used to gauge the task-independent state of the network. Results of both methods were investigated as predictors of N100 response to S1 and N100 suppression from S1 to S2, thus improving the specificity of mapping DMN network properties to ERP abnormalities in SZ.

Method

Participants

52 SZ and 25 HC had EEG from the paired stimulus paradigm necessary for calculation of N100 ERP measures and task-based oscillatory coherence analyses.

Measures

EEG Procedures.

Participants completed a standard paired-stimulus, or "paired S1-S2," task during which they were presented with 160 trials of two identical auditory stimuli, S1 and S2, that were 3 ms in duration, with a 500 ms ISI and a variable 9-11 s between pairs. Auditory stimuli were

presented through in-ear headphones at 76 dB assessed via decibel meter. To confirm normal hearing, a brief screening test was conducted at the start of each session. EEG was recorded as previously described under Study Aim 1, and pre-processing of EEG data generally followed the steps previously outlined. Data underwent further artifact rejection using the artifact scanning tool of BESA. Trials containing artifacts (amplitude > 90 μV, gradients > 46 μV/sample) were rejected, and only participants with at least 60 trials of EEG data after artifact rejection were included in subsequent analyses. 9 SZ and 2 HC were excluded due to insufficient number of trials providing the final set of 52 SZ and 25 HC (see Table 2).

N100 component analysis.

N100 amplitude was scored from the Cz channel. N100 to S1 and S2 was identified using an automatic peak-detection algorithm within a 50-150 ms post-stimulus window. A high-pass 1 Hz, forward, 6 dB/octave and low-pass 20 Hz, zero-phase-shift, 24 dB/octave bandpass filter was used for scoring of N100. Accuracy of automated scoring was subsequently confirmed by visual inspection. N100 amplitude to S1 was scored relative to baseline (-200 – 0 ms). N100 ratios were restricted to a range from zero (complete suppression of response to S2) to 2, such that values larger than 2 were truncated so that outliers would not have a disproportionate effect on group means. Lower N100 ratio scores are interpreted to reflect more intact inhibitory gating.

MRI Procedures.

Methods were the same as those described under Study Aim 1.

DMN Suppression Analyses

Definition and assessment of DMN using fMRI and EEG data generally followed the procedures outlined in Study Aim 1. Complex demodulation was used for time-frequency analyses using EEG data with a time-frequency sampling of 1 Hz, 50 ms within an epoch of -

6000 ms to 3000 ms around presentation of S1. To assess suppression of DMN during the S1-S2 paradigm, time-frequency representations of scalp EEG data during pre-stimulus (-2 – -0.25 seconds) and post-stimulus (0-2 seconds) periods were evaluated. Suppression of intra-network DMN connectivity from pre- to post-stimulus was calculated for each participant using estimates of imaginary, frequency-resolved coherence between 2 and 40 Hz. Coherence was computed between nodes of DMN and used as a measure of intra-network DMN connectivity. DMN suppression during the paired-stimulus paradigm was assessed by examining baseline-adjusted (pre-S1) intra-network DMN coherence following S1. Group differences (SZ, HC) were assessed using cluster-based permutation testing. Average coherence for each participant within identified clusters was extracted and used to quantify pre- to post-stimulus intra-DMN changes (e.g., suppression).

The main effect of pre- to post-stimulus DMN suppression on S1 N100 amplitude and the N100 ratio score was examined as well as the interaction between DMN suppression and group. Exploratory analyses were conducted using the PROCESS macro for SPSS (Hayes, 2012) to identify possible mediation of the effect of group (SZ, HC) on S1 N100 amplitude and the N100 ratio score by pre- to post-stimulus DMN suppression. Inferences were made using 10,000 bootstrap estimates to generate a 95% confidence interval for calculation of mediation effects, and the null hypothesis was rejected if the 95% confidence intervals for the indirect effects did not include zero. This method was adopted because, unlike the Sobel test, it makes no assumptions about the shape of the sampling distribution of the indirect effect (Hayes, 2017). It is also one of the higher-powered approaches to inference in mediation modeling and is based on an estimate of the indirect effect itself, in contrast to the causal steps approach.

Similar analyses were computed using intra-network DMN connectivity from rs-EEG and rs-fMRI data to examine the main effect of intrinsic resting state DMN connectivity on N100 variables, the interaction of intrinsic DMN connectivity and group (SZ vs HC), and potential mediation of the effect of patient status on N100 by DMN suppression.

Results

Participant Data

There were no significant differences on demographic measures between SZ and HC participants included in Study Aim 2 analyses.

N100 Variables

Grand-average ERP waveforms for each group are shown in Figure 7A. Consistent with prior reports, HC exhibited larger (i.e., more negative) N100 amplitude to S1 than SZ (*t(75) = 2.9, p = 0.005;* Figure 7B) and to S2 (*t(75) =2.6, p = 0.01;* Figure 7C*).* An overall suppression effect was observed, with N100 amplitude to S2 significantly attenuated compared to S1 (*t(76)= 5.4, p <0.001)*. To evaluate the extent to which N100 suppression in each group reflected the response elicited by each stimulus and to provide a difference measure of N100 suppression, a repeated-measures ANOVA was conducted with Group (SZ, HC) and Stimulus (S1, S2) factors. Results indicated main effects of Group (*F(1, 75) = 32, p = <0.001*) and Stimulus (*F(1, 75) = 10.6, p = 0.002*) as well as a marginal Group*Stimulus interaction (*F(1, 75) = 2.5, p = 0.1*). A trending group difference was similarly found for the N100 ratio score, such that SZ demonstrated impaired suppression (i.e., higher ratios) than HC (*t(75) =1.7, p = 0.1;* Figure 7D*).*

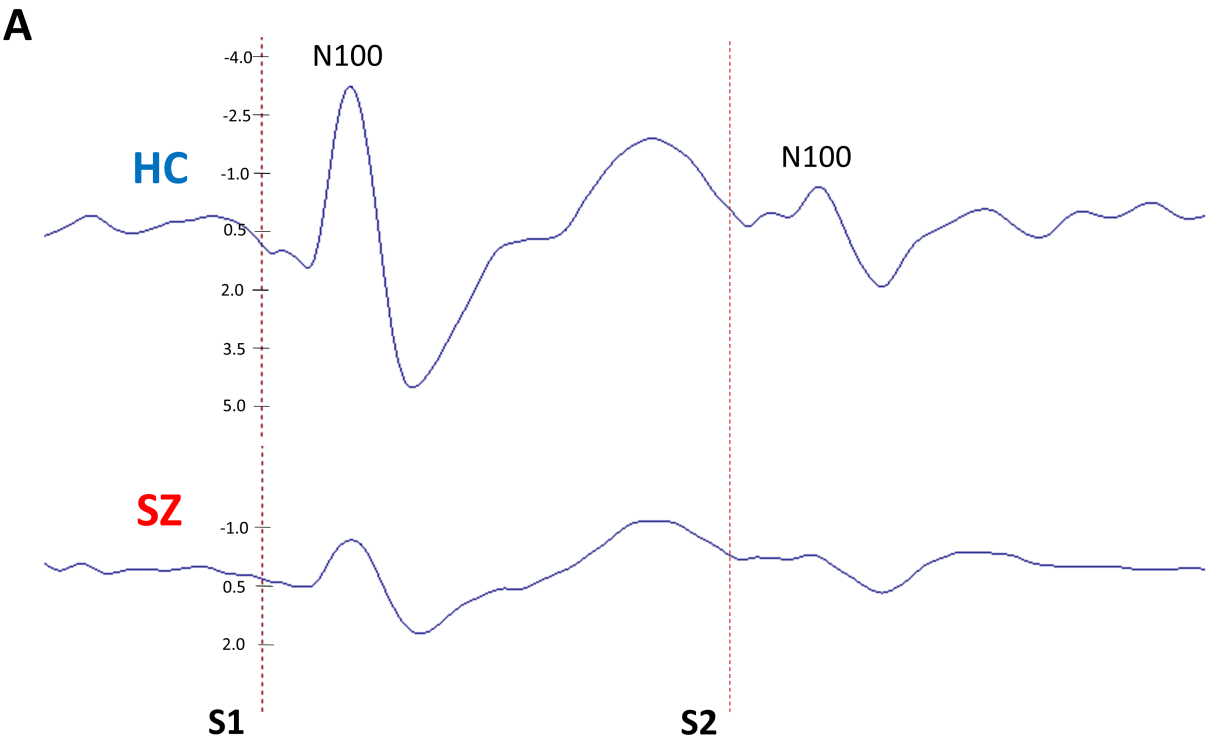
A
N100
N100
HC
SZ
-4.0
-2.5
-1.0
0.5
2.0
3.5
5.0
-1.0
0.5
2.0
S1
S2

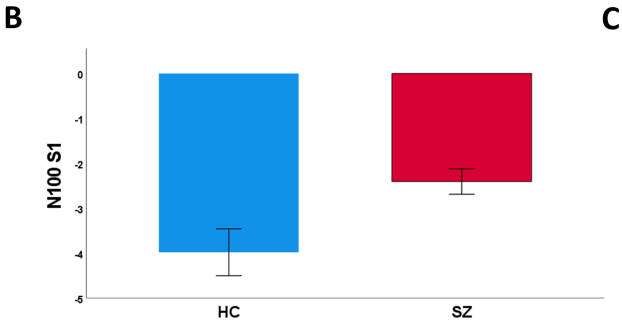
B
N100 S1
0
-1
-2
-3
-4
-5
HC
SZ

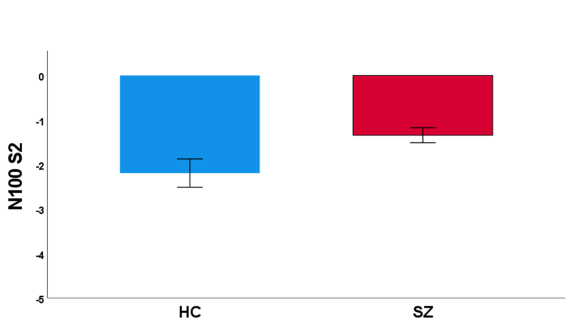
C
N100 S2
0
-1
-2
-3
-4
-5
HC
SZ

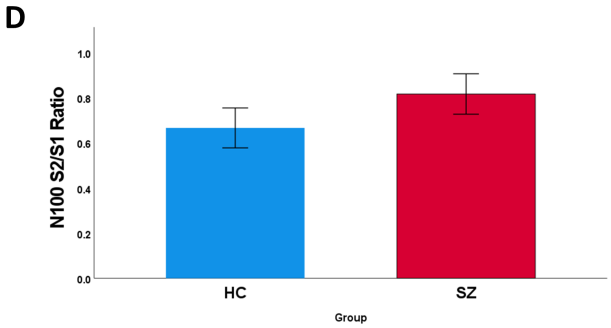
D
N100 S2/S1 Ratio
1.0
0.8
0.6
0.4
0.2
0.0
HC
SZ
Group

Figure 7. Group (SZ, HC) differences in N100 variables. A) Grand-average waveforms for HC and SZ recorded at Cz. X-axis spans time 250 ms pre-S1 to 1000 ms post-S1. Y-axis in microvolts. B) HC (blue) participants demonstrate larger (more negative) N100 amplitude to S1 than do SZ (red) patients. C) HC demonstrate larger (more negative) N100 S2 amplitude than do SZ. D). SZ demonstrate larger N100 ratio scores than do HC (trending effect). Error bars denote +/- SE

Task-based EEG-derived DMN Coherence

Contrary to hypotheses, SZ demonstrated less intra-DMN connectivity (*M = .14, SD = .17*) than HC (*M = .36, SD = 0.32*) during the paired S1-S2 paradigm, as exhibited by less coherence in the 4-7 Hz (theta) range immediately following S1 onset (0.1-0.6 seconds; Figure 8a). Average coherence was extracted from this cluster for each participant and within this cluster, the size of the effect was large (*t(75) = 3.9, p < 0.001, d = 0.95*; Figure 8b).

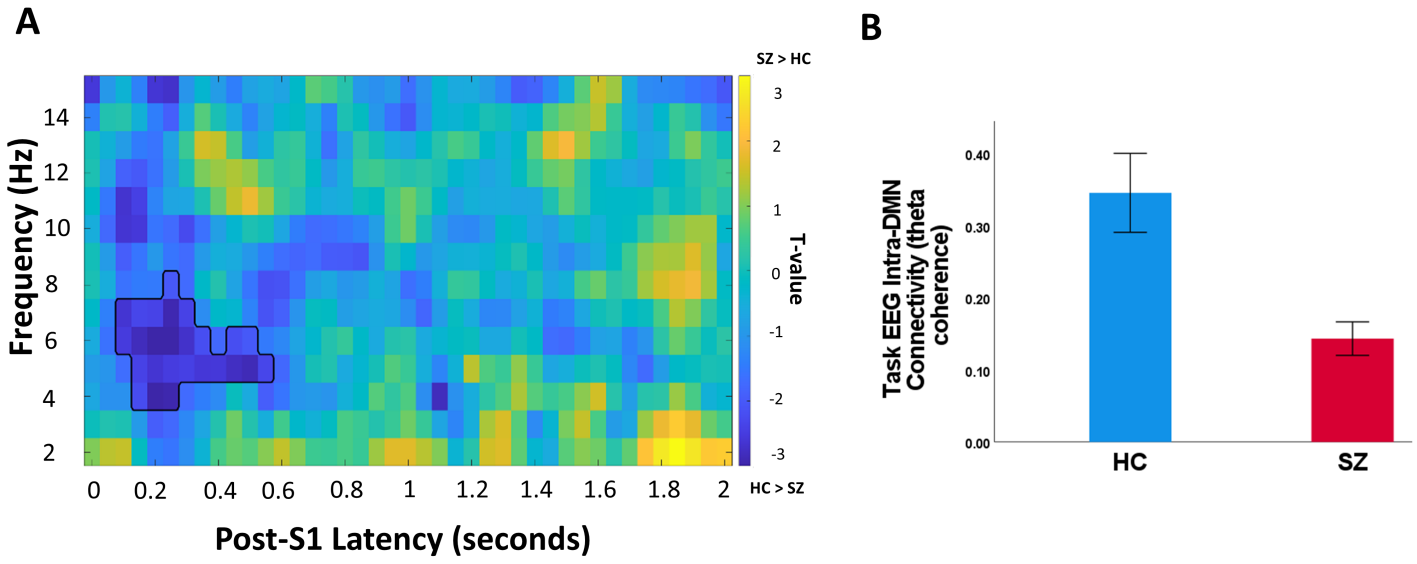

Figure 8. Group (SZ, HC) differences in baseline-adjusted (pre-stimulus) intra-DMN coherence during paired S1-S2 task. A) Blue (negative t-values) cluster between 4-7 Hz, outlined in black, denotes greater coherence in HC than SZ following S1 onset. B) Extracted average coherence within the highlighted 4-7 Hz theta-band cluster. for SZ (red) and HC (blue). Error bars denote +/- SE.

Average coherence within this cluster did not predict N100 amplitude to S1 *(β = -.1, t(75) = 0.9, p = 0.4)* or N100 suppression *(β = 0.03, t(75) = 0.3, p = 0.8).* There also was no interaction effect involving Group and coherence within this cluster for N100 amplitude to S1 *(β = 0.2, t(73) = 1.1, p = 0.3)* or the N100 ratio score *(β =0.07, t(73) = 0.4, p = 0.7).*

Analyses examining possible mediation of the effect of Group on N100 variables by task-based intra-DMN connectivity using EEG coherence yielded non-significant indirect effects. Group status did not influence N100 amplitude to S1 *(-0.08, CI = -0.7 to 0.5*) or the N100 ratio score *(-0.04, CI = -0.2 to 0.1*) indirectly through task-based intra-DMN connectivity.

rs-fMRI-derived DMN Connectivity

There was no association between rs-fMRI-derived intra-DMN connectivity and N100 amplitude to S1during the paired-stimulus paradigm *(β = -.1, t(39) = 0.7, p = 0.5).* However, an interaction between Group and intra-DMN connectivity on N100 amplitude to S1 was detected *(β = 1.6, t(37) = 4.4, p = 0<0.001),* such that SZ exhibiting more resting state intra-DMN connectivity showed an attenuated N100 to S1 (*r(20) = 0.5, p = 0.04*), whereas HC demonstrated the opposite pattern (*r(21)= -0.6, p = 0.003*; Figure 9).

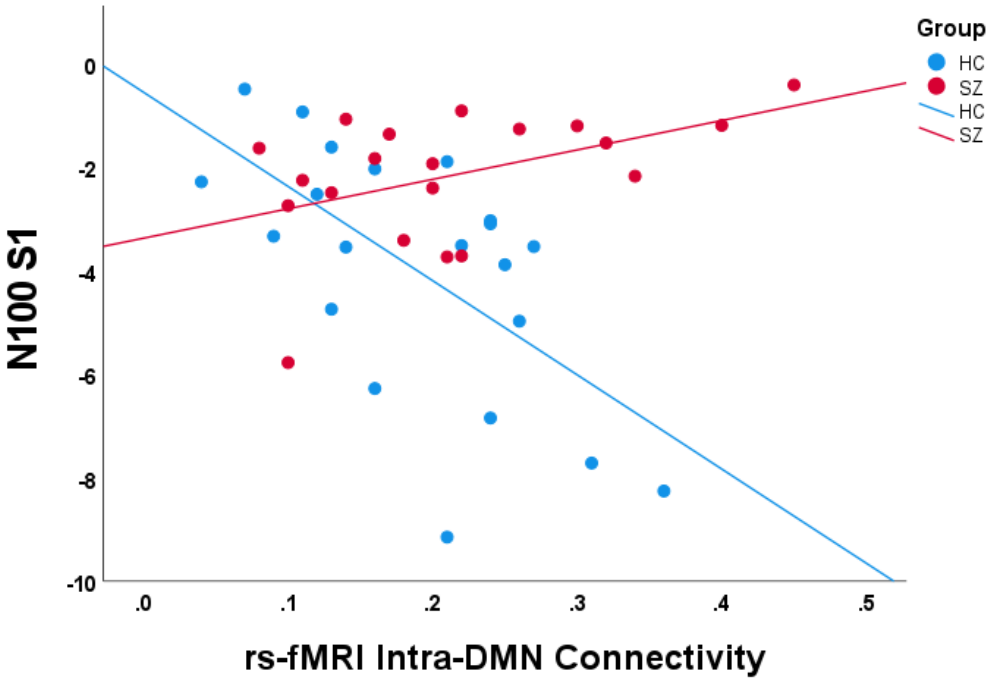

Figure 9. Relationship between intra-DMN connectivity assessed using rs-fMRI data, on the x-axis, and N100 amplitude to S1, shown in microvolts on the y-axis. A Group*DMN Connectivity interaction was found such that SZ (red) exhibiting higher resting state intra-DMN connectivity demonstrated lower (less negative) N100 amplitude to S1, whereas HC (blue) showed the opposite pattern.

Similarly, resting state intra-DMN connectivity did not predict the N100 ratio score *(β = 0.09, t(39) = 0.5, p = 0.6).* A trending interaction between Group and resting state intra-DMN connectivity on N100 suppression was found *(β = 0.8, t(37) = 1.8, p = 0.09;* Figure 10*)* such that SZ exhibiting greater intra-DMN connectivity tended to demonstrate larger N100 ratios (i.e., less suppression; *r(20)= 0.3, p =0.2*), whereas HC tended to exhibit the opposite pattern of results (*r(21) = -0.3, p = 0.2*), although these relationships were not statistically significant.

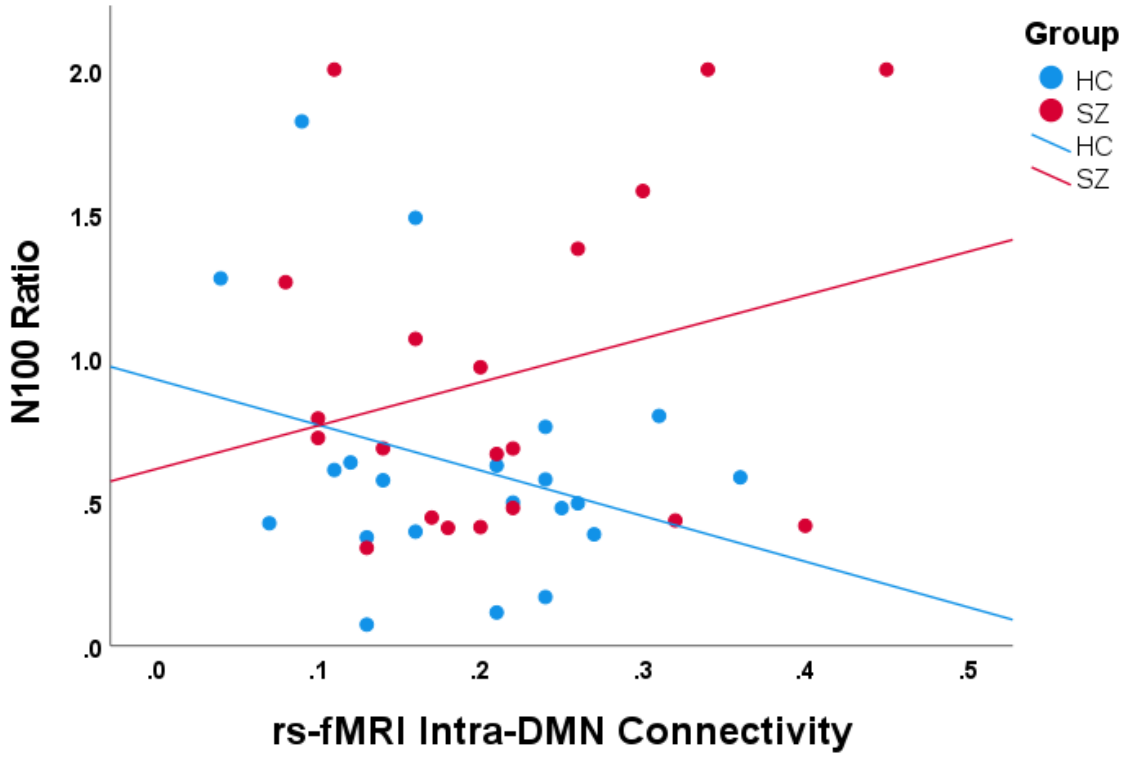

Figure 10. Group (SZ, HC) differences in relationship between intra-DMN connectivity assessed using rs-fMRI data, on the x-axis, and N100 ratio score (S2/S1), on the y-axis. A Group*DMN Connectivity interaction was found such that SZ (red) exhibiting greater resting state intra-DMN connectivity demonstrated higher N100 ratios, whereas HC (blue) showed the opposite pattern.

Analyses examining possible mediation of the effect of Group on N100 variables by rs-fMRI-derived intra-DMN connectivity did not reveal significant indirect effects. Group status did not influence N100 amplitude to S1 *(-0.1, CI = -0.5 to 0.3*) or the N100 ratio score *(-0.007, CI = -0.07 to 0.1*) indirectly through resting state intra-DMN connectivity.

rs-EEG-derived DMN connectivity

As a multimodal replication of rs-fMRI findings, the relationship between intra-network resting state DMN connectivity using EEG coherence and N100 amplitude to S1 was examined. There was no main effect of intra-DMN connectivity using EEG data on N100 amplitude to S1

(β = 0.04, t(50)=0.3, p = 0.8), nor was there an interaction between Group and intra-DMN beta coherence *(β = 0.2, t(47)=1.0, p = 0.3)*. Furthermore, average coherence within this cluster did not predict N100 suppression (*t(49) = 1.1, p = 0.3).* However, there was an interaction between Group and resting state intra-DMN connectivity for N100 suppression *(β = 0.3*, *t(47) = 2.2, p = 0.03;* Figure 11*)*, such that greater resting state intra-DMN coherence tended to be associated with higher N100 ratio scores in SZ (*r(26) = 0.2, p = 0.4*), whereas the opposite pattern was observed in HC (*r(25) = -0.2, p = 0.3*); neither slope differed from zero.

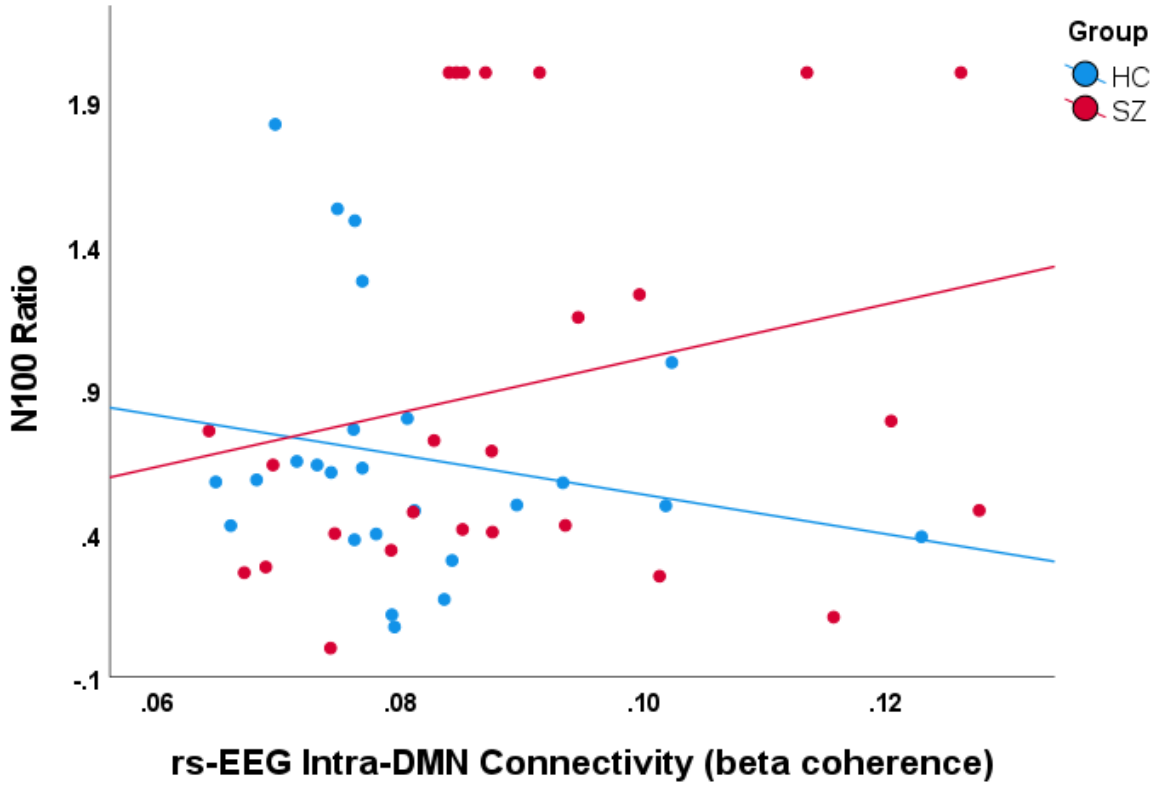

Figure 11. Group (SZ, HC) differences in relationship between intra-DMN resting state coherence, on the x-axis, and N100 ratio score, on the y-axis. A Group*DMN Connectivity interaction was found such that SZ (red) exhibiting greater resting state intra-DMN coherence demonstrated higher N100 ratios, whereas HC (blue) showed the opposite pattern.

Analyses examining possible mediation of the effect of Group on both N100 variables by resting state intra-DMN connectivity using EEG coherence also failed to demonstrate significant indirect effects. Group status did not influence N100 amplitude to S1 *(-0.05, CI = -0.7 to 0.4*) or N100 ratio scores (*0.04, CI = -0.1 to 0.2*) indirectly through resting state intra-DMN coherence.

Relationship Between Resting-State and Task-based DMN Connectivity Measures

Relationships were computed between resting-state and task-based DMN connectivity measures in order to determine whether the same SZ were demonstrating abnormalities across all three measures or instead these measures were capturing separate phenomena or distinct profiles of dysfunction in SZ . Resting state intra-DMN connectivity (beta coherence) and intra-DMN connectivity during the paired S1-S2 paradigm (theta coherence) were not correlated (*r(51) = 0.09, p = 0.5*). Furthermore, SZ and HC did not differ in their relationship between rest- and task-based intra-DMN connectivity measures *(β = -1.2, t(47) = 1.5, p=0.2*; Figure 12). The absence of an association was confirmed by follow-up simple-slopes analysis between intra-DMN connectivity measures in SZ *(β = -.1, t(24) = 0.7, p = 0.5*).

Resting state intra-DMN connectivity using fMRI data and intra-DMN connectivity using EEG coherence during the paired S1-S2 paradigm were also not correlated (*r(41) = -0.2, p = 0.3*). SZ and HC did not differ in their relationship between task and rest-based intra-DMN measures *(β = -.2, t(37) = 0.4, p= 0.7*; Figure 13).

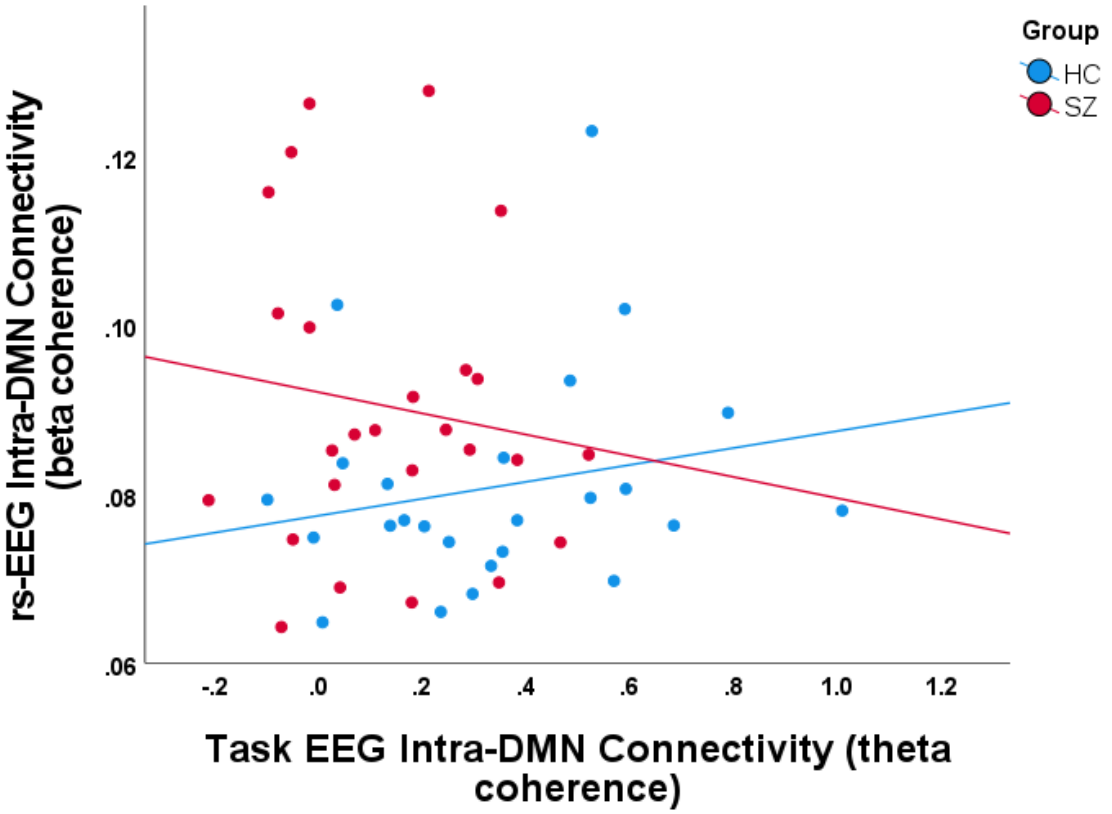

Figure 12. Relationships between task-based EEG connectivity, on the x-axis, and resting state EEG connectivity, on the y-axis, assessed with coherence. Intra-DMN coherence at rest (beta) and during the paired S1-S2 (theta) were not correlated. Neither SZ (red) nor HC (blue) demonstrated significant relationships between these coherence measures.

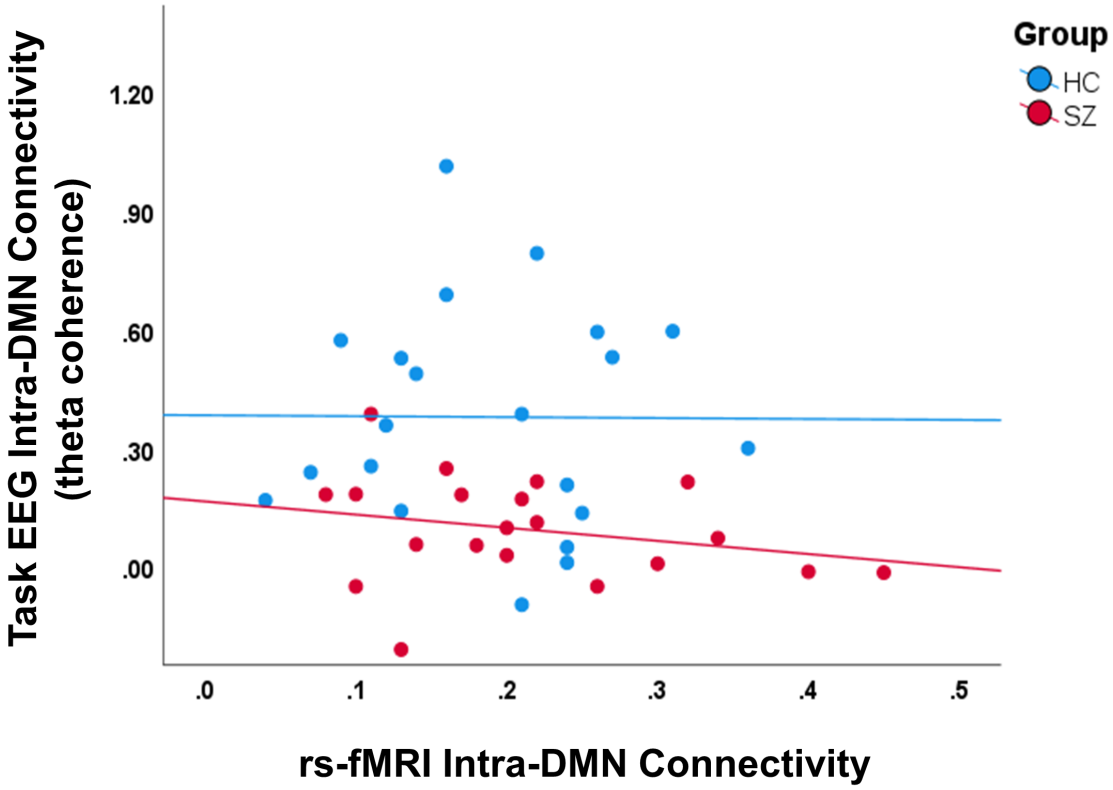

Figure 13. Relationships between resting state intra-DMN connectivity using fMRI, on the x-axis, and task-based intra-DMN connectivity using EEG coherence, on the y-axis. Intra-DMN connectivity at rest assessed with fMRI data and intra-DMN coherence during the paired S1-S2 (theta) assessed with EEG oscillatory data were not correlated. Neither SZ (red) nor HC (blue) demonstrated significant relationships between these connectivity measures.

Multimodal Data Fusion: rs-EEG- and rs-fMRI-derived Intra-DMN Connectivity Relationships with N100 Variables

In order to evaluate the unique and shared variance in the N100 variables captured by rs-EEG-derived and rs-fMRI-derived DMN connectivity, hierarchical regressions were conducted with these connectivity measures as predictors of N100 amplitude to S1 and the N100 ratio

score. For N100 amplitude, the full model including all predictors (Group, rs-EEG-derived DMN Connectivity, rs-fMRI-derived DMN Connectivity) and all interactions accounted for 48% of the variance (*F(7,23) = 3.1, p = 0.02*). Neither rs-EEG (*ΔR^2 = 0.003, b = 0.06, t = 0.3, p =0.8*) nor rs-fMRI (*ΔR^2 = 0.07, b = -0.3, t = 1.5, p =0.1*) connectivity, when added third to the model, contributed unique variance. Evaluating unique variance contributed by the two two-way interactions of interest, the Group*rs-MRI-derived DMN interaction provided $\Delta R^2 = 0.3$ *(b = 1.3, t = 3.4, p =0.002*). The Group*rs-EEG-derived DMN interaction added little (*ΔR^2 = 0.01, b = -0.7, t = 0.7, p =0.5*).

Discussion

The overarching goal of Study Aim 2 was to determine whether suppression of DMN supports attention allocation, as indexed by N100 amplitude to S1, and/or inhibitory processing, as reflected by the N100 suppression ratio. Because cognitive functions are subserved by the activity of interacting brain regions, clarifying the neural networks involved in salience and inhibitory processing as indexed by N100 during the paired S1-S2 paradigm can provide insights into the mechanisms supporting these processes. Contrary to hypotheses, SZ demonstrated less evoked intra-DMN connectivity than HC as evidenced by less baseline-adjusted theta coherence following presentation of S1. Observation of decreased intra-DMN connectivity following S1 suggests that, rather than insufficient task-related DMN suppression as hypothesized, SZ may actually demonstrate abnormalities in task-evoked DMN functions triggered by the stimuli presented during the S1-S2 paradigm. Despite these group differences, intra-DMN connectivity during the paired S1-S2 did not predict either N100 variable, suggesting that this connectivity instead captured other cognitive processes associated with the task.

The majority of prior research indicates that DMN suppression during experimental tasks supports disengagement from distracting, introspective processing (Chadick & Gazzaley, 2011) and promotes task performance (Weissman et al., 2006; Anticevic et al., 2010). However, a developing line of research suggests that DMN may actually be involved in fulfilling cognitive demands during various tasks. Rather than DMN activity generally interfering with task-related cognitive processing, DMN may actually be involved in the neural response to the stimuli presented during the S1-S2 paradigm (e.g., Vatansever et al., 2015). Within this framework, regions of DMN flexibly respond to cognitive demands and contribute to task performance through global integration of information in order to adapt to a diverse range of tasks. It has been suggested that the activity of DMN is made up of overlapping neural signals from other large-scale neural networks and that the summation of these signals over time produces what is observed as DMN (Smith et al., 2012). Braga and colleagues (2013) suggest that nodes of DMN are placed in such a way as to modulate communication between other functional networks and to integrate information exchanged between these networks.

Findings from the present study are consistent with the interpretation that SZ exhibit less cross-node communication in DMN during the paired S1-S2 paradigm than HC, despite findings of resting state DMN hyperconnectivity as observed in Study Aim 1 and by others (e.g., Hu et al., 2017). The conceptualization of disengagement of DMN during externally-focused paradigms or tasks is likely oversimplified, as present findings suggest that S1-S2 stimuli fostered intra-DMN connectivity in HC but not in SZ. Present findings of evoked-DMN connectivity differences between SZ and HC during the task were observed in the theta frequency range. Theta-band activity has been implicated in various functions including cognitive control (Cavanaugh & Frank, 2014), short-term memory (Klimesch et al., 1997), and

divided attention (Keller et al., 2017). Previous work has demonstrated resting state theta-band DMN abnormalities in SZ (e.g., Andreou et al., 2015; Krukow et al., 2020; Nakhnikian et al., 2021), but to our knowledge this is the first study to demonstrate task-based theta-band DMN alterations in the disorder.

Consistent with the network integration hypothesis described above, theta connectivity in DMN may reflect integration of information from other networks elicited by the paired auditory stimuli, such as the frontoparietal control network (FPCN). Function of FPCN has been linked to theta oscillations (Kam et al., 2019; Helfrich et al., 2018). This hypothesis aligns with a study that found that DMN-FPCN coupling was increased during goal-directed cognitive processing (Spreng et al., 2010). Thus, present findings of decreased theta DMN connectivity among SZ during the S1-S2 paradigm may reflect dysfunction in DMN-FPCN network integration. Future research could examine intrinsic and task-based DMN-FPCN network dynamics to clarify this potential mechanism of cognitive processing as well as dysfunction of this mechanism in SZ.

It was also expected that intra-DMN connectivity during the paired-stimulus paradigm would predict N100 variables. Alterations in intra-DMN theta-band coherence following the onset of S1 in SZ were not found to be associated with N100 activity measured in the present study, however. Given the purported role of theta in encoding of new information (Klimesch et al., 1999) and working memory (Hsieh et al., 2011; Roux & Uhlhaas, 2014; Sauseng et al., 2004; Sauseng et al., 2010), the triggering of attention manifested in N100 may be supported by a different neural mechanism of attention. Decreased theta-band DMN coherence in SZ may instead predict working memory deficits, which have been commonly cited in SZ (for a review, see Forbes et al., 2009). Evaluation of DMN during a working memory task, such as the N-back

(Kirchner, 1958), could serve to clarify the specific cognitive function of DMN theta connectivity and associated dysfunction in SZ.

Additionally, it was predicted that SZ would exhibit higher N100 ratios than HC as has been shown previously (Brockhaus-Dumke et al., 2008; Boutros et al., 2009). N100 ratios were higher in SZ than HC in the present study, although with marginal significance. The directional a priori hypothesis of higher N100 ratios in SZ in the present study would generally justify a 1-tailed statistical test, with which this finding would be considered on the cusp of significance at the $p < 0.05$ level. Present findings align with a recent meta-analysis that found that alterations in N100 amplitude to S1 are more reliably observed in SZ than N100 suppression abnormalities (Rosburg et al., 2018). Hsieh and colleagues (2012) assessed auditory ERPs in a sample including FE SZ, ultra-high risk, early/broad at-risk mental states, and HC. A monotonic gradient of increasing gating deficits was found across the different levels of clinical severity. This finding suggests that N100 suppression deficits and associated cognitive dysfunction are more commonly observed in later stages of psychosis than are captured in the present sample of FE SZ.

In order to determine whether the same individuals in the SZ group were demonstrating abnormal DMN connectivity in the resting state and during the S1-S2 paradigm, relationships between these measures were assessed. If the same individuals demonstrate resting state hyperconnectivity and task-based hypoconnectivity of DMN, it would support the theory that DMN hyperconnectivity in the resting state represents a compensatory mechanism in response to generalized functional dysconnectivity in the disorder. Intra-DMN connectivity at rest and during the task were not significantly related across all participants or specifically in either group. This finding suggests that, rather than the same SZ demonstrating aberrant intra-DMN connectivity

during resting state and during the paired-stimulus paradigm, two distinct profiles of abnormal DMN connectivity may be present. Further, assessment with oscillatory EEG data shows that these profiles correspond to different frequency bands—beta at rest and theta during the task. These profiles of abnormal DMN function may reflect specific pathogenic processes associated with distinct alterations of neural network function in SZ. It seems likely that these DMN profiles differentially predict cognitive deficits and symptoms in SZ, or SZ subgroups, and may respond to different targeted interventions.

Moderation and exploratory mediation analyses were conducted because it was unclear whether SZ and HC would demonstrate different relationships between DMN connectivity and N100 variables, or whether SZ would exhibit alterations in DMN connectivity, which would in turn predict abnormal N100 responses. In the present study, SZ and HC generally demonstrated opposing relationships between resting state DMN connectivity and N100 variables, such that greater intra-DMN connectivity was associated with attenuated N100 amplitude and higher N100 ratio scores in SZ. These Group*DMN connectivity interactions suggest that SZ and HC have different relationships between intrinsic DMN connectivity and the attentional processes assessed with N100, rather than supporting a model wherein the effect of patient status on N100 is mediated by alterations in intrinsic DMN function.

Although SZ and HC differed in their relationships between resting state DMN connectivity and the N100 ratio score, no interaction or mediation effects were found using task-based DMN connectivity for either N100 variable. Task-based DMN abnormalities in SZ may alternatively correspond to dysfunction in other cognitive processes that were not assessed in the present study, such as working memory as discussed above. It would be valuable in future

research to delineate the mechanisms through which alterations in DMN connectivity contribute to SZ and in which contexts these alterations are observed (e.g. during a task vs. at rest).

Due to the complexity of dysfunction in SZ, it is unlikely that a single measurement modality could provide comprehensive knowledge of the phenomena of interest (Lahat et al., 2015). DMN connectivity assessed with both EEG and fMRI data in the present study provided means for multimodal data fusion, which not only aids in clarifying common vs. unique signal properties across modalities but provides a means for unifying and refining models of disorder-related dysfunction. A primary goal of Study Aim 2 was to utilize multimodal data fusion to elucidate the relationships between different methods for assessing salience and inhibitory processing abnormalities in SZ and to clarify the nature of dysfunction in the mechanisms supporting these processes. Simple correlation (see Study Aim 1) demonstrated that resting state EEG and fMRI DMN measures were positively related ($r = 0.4$) across all participants, with no group differences in this relationship. When both connectivity measures were entered together as predictors of N100 amplitude and the N100 ratio score, main effects for either DMN measure were not significant. Together, these results suggest that EEG and fMRI assessments of resting state intra-DMN connectivity are capturing, to some extent, the same DMN phenomenon and its relationship with N100 variables. However, the interaction between group and resting state DMN connectivity assessed with fMRI contributed unique variance in regression models predicting N100 ratio. This pattern of results indicates that these multimodal measures of DMN connectivity, though related, are not fully redundant.

The distinct variance in DMN function captured by each of these two modalities may contribute to discrepancies that arise between findings in the fMRI and EEG literatures. fMRI-derived DMN may be capturing disorder-related DMN phenomena that the EEG-derived DMN

connectivity is missing. This may be related to differences in temporal and spatial resolution between oscillatory EEG and fMRI connectivity measures. Alternatively, EEG and fMRI measures of DMN connectivity may not represent equivalent measures of these N100 processes. One hypothesis is that EEG- and fMRI-derived measures of resting state DMN connectivity are capturing some shared aspects of what N100 amplitude and the N100 ratio score reflect, with fMRI capturing unique aspects of this construct that were not observed using EEG in the present study. Continued multimodal evaluation with a larger sample could clarify the unique and shared characteristics of salience and inhibitory processing abnormalities in SZ that can be assessed using each modality.

In summary, contrary to theories that suggest DMN disengagement is wholly beneficial to task performance, findings from Study Aim 2 suggest that this conceptualization of DMN's role is oversimplified. Rather, specific DMN functions may support the cognitive processes elicited during the paired-stimulus paradigm. Although task-based DMN connectivity did not predict N100 variables, resting state measures of DMN connectivity across both EEG and fMRI modalities suggest that SZ differ from HC in their relationship between intrinsic DMN connectivity and N100. Multimodal data fusion analyses demonstrated that EEG and fMRI assessments of resting state DMN connectivity were related, although these measures appear to capture different aspects of N100 phenomena associated with SZ. Due to possible limitations with regard to power in the present study, future work should continue to assess these relationships with larger samples.

Study Aim 3: Evaluate differences in SAL down-regulation of DMN between FE SZ and HC, and determine whether SAL down-regulation of DMN represents a mechanism supporting salience and inhibitory processing

Although considerable research has been dedicated to understanding attention, the manner in which relevant stimuli are selected for additional processing remains unclear. One theory of selective attention suggests that two primary mechanisms are involved in this process: 1) amplification of targets, and 2) inhibition of distractors (Tipper et al., 1994; Wyatt & Machado, 2013; Yeshurun & Carrasco, 1998). Each mechanism is proposed as a distinct component that works independently of the other (Bidet-Caulet et al., 2010), although the exact temporal relationship between the two processes has yet to be determined. Houghton and Tipper (1994) suggest that selection of inputs for additional processing among competing stimuli occurs via matching of expectations produced by top-down processes (e.g., expectation of the to-be-attended stimulus) with bottom-up perceptual inputs. A positive feedback loop is initiated to increase processing in the case of a match, whereas a negative (inhibitory) feedback loop is activated if inputs fail to match. In the present study, amplification of relevant stimuli aligns closely with how salience processing by the SAL network is conceptualized. Specifically, interactions between regions of SAL are understood as forming an information processing loop for responding to salient internal or external stimuli and amplifying them (Seeley, 2019) via communication with other large-scale networks, such as DMN, to facilitate access to attentional resources when a salient event is detected (Menon & Uddin, 2010). Because SAL is purported to play a causal role in influencing DMN in order to focus the "spotlight of attention" on externally-focused tasks, effective down-regulation of DMN by SAL is critical for effective salience

processing and cognitive function. Therefore, SAL-DMN dynamics are posited to correspond both to the amplification of relevant information and to the initiation of an inhibitory feedback loop for irrelevant or distracting information.

Given the theorized roles of, and communication between, DMN and SAL, the direction and strength of effective connectivity between these networks were expected to predict N100 amplitude to S1 and N100 suppression. Specifically, it was hypothesized that greater SAL-to-DMN directed connectivity would be associated with larger N100 amplitude to S1 and enhanced N100 suppression. Hare and colleagues (2019) found that SZ demonstrate greater directed DMN-to-SAL connectivity, and the extent of this connectivity predicted positive and negative psychotic symptoms. In the present study, it was expected that SZ would similarly demonstrate greater DMN-to-SAL directed connectivity than HC, thereby influencing determination of what is judged salient.

To examine directed (effective) connectivity, Granger causality (GC) analysis was used to quantify connectivity between DMN and SAL during the S1-S2 paradigm and during resting state using EEG and fMRI data. GC facilitates the identification of directional interactions from time series data, providing important network-operation information beyond identifying the shape of functional neural networks typically identified using traditional functional connectivity analyses. GC analysis statistically identifies potential causality based on prediction under the theory that signal X "Granger causes" signal Y if the past values of X contain information that predicts Y over and above the information provided in the past values of Y alone (Astolfi et al., 2007; Barnett et al., 2009; Granger, 1969). This follows from the premise that a cause cannot follow an effect. Accordingly, prediction error for the model including both X and Y was compared to prediction error for the model containing only Y. If the prediction error is reduced

by the incorporation of preceding values of X, then X is said to have a Granger causal influence on Y.

Method

Participants

fMRI data collected from 38 SZ and 20 HC were included for resting state GC analyses while EEG data for GC during the paired-stimulus paradigm were available for 52 SZ and 25 HC (see Table 2).

Measures

EEG Procedures.

Data acquisition and processing were completed using the methods described under Study Aims 1 and 2.

MRI Procedures.

The methods for data collection and processing were the same as those described under Study Aim 1.

Multimodal Evaluation of DMN and SAL

Evaluation of SAL using EEG and fMRI data generally followed procedures outlined for assessment of DMN in Study Aim 1. Spectrally resolved GC analysis using BESA Connectivity was used to evaluate the directionality of inter-network connectivity (i.e., effective connectivity) in EEG data (Geweke et al., 1982). Analysis of GC using rs-fMRI data generally followed the methods of Luo et al. (2013) and Guha et al. (2019). Average blood-oxygen-level dependent (BOLD) signals were extracted for each network, detrended, and zero-centered prior to GC

analysis. Using a vector autoregressive (AR) model for GC, the GC influence of X to Y was quantified as

$$F_{x \to y} = \log\left[\frac{\det(\sum y)}{\det(\sum yx)}\right],$$

When the value of $F_{x \to y}$ is greater than 0, GC from X to Y is indicated, whereas a value of 0 indicates otherwise. A log likelihood ratio test was then used for causal inference. This statistic is approximately $\chi 2$-distributed with degrees of freedom equal to $2d_x d_y$ where dx and dy are the dimensions of the column vectors representing the time courses of X and Y. Because research suggests that the variation of the BOLD time series across trials increases with the magnitude of the signal, an approach accounting for signal-dependent noise was employed (Luo et al., 2013).

Simulation studies applying GC to fMRI data have shown that for sampling periods longer than 500 ms a lag of one is optimal (Bressler et al., 2008; Roebroeck et al., 2005; Wen et al., 2012). To maximize the stability of the AR model, and because the sampling period (repetition time, or TR) of the rs-fMRI data for this study was 800 ms, a first-order (lag-one) model was used.

In order to address hypotheses directly and to reduce the number of computed regressions, both directions of causality within the DMN-SAL circuit (DMN-to-SAL and SAL-to-DMN) were combined via "GC asymmetry" scores computed by subtracting the log-likelihood of SAL-to-DMN GC from the log-likelihood of DMN-to-SAL GC. As such, a higher GC asymmetry score denotes greater directed connectivity from DMN to SAL than from SAL to DMN. GC asymmetry scores were transformed using Lambert Way to Gaussianize (Goerg, 2015).

The main effect of DMN-SAL connectivity on N100 variables was examined as well as the interaction between group and DMN-SAL connectivity. Exploratory analyses were conducted to

identify possible mediation of the effect of group N100 amplitude to S1 and the N100 ratio score by DMN-SN connectivity.

Results

Participant Data

Demographic information for participants can be found in the Method sections of Study Aim 1 (participants included in resting state connectivity analyses) and Aim 2 (participants included in task-based connectivity and ERP analyses). No significant group differences were found for any of the demographic variables.

Task-based EEG-derived DMN-SAL GC

No group differences in effective connectivity between DMN and SAL were identified in the rest or paired S1-S2 oscillatory EEG data.

rs-fMRI-derived DMN-SAL GC

SZ demonstrated greater resting state DMN-to-SAL GC than HC ($t(39)=2.1, p = 0.04$), although HC did not exhibit greater SAL-to-DMN GC ($t(39) = 0.6, p = 0.3$). GC asymmetry scores demonstrated that SZ exhibited greater resting state DMN-to-SAL GC relative to SAL-to-DMN than HC ($t(39) =2.4, p = 0.03;$ Figure 14*)*.

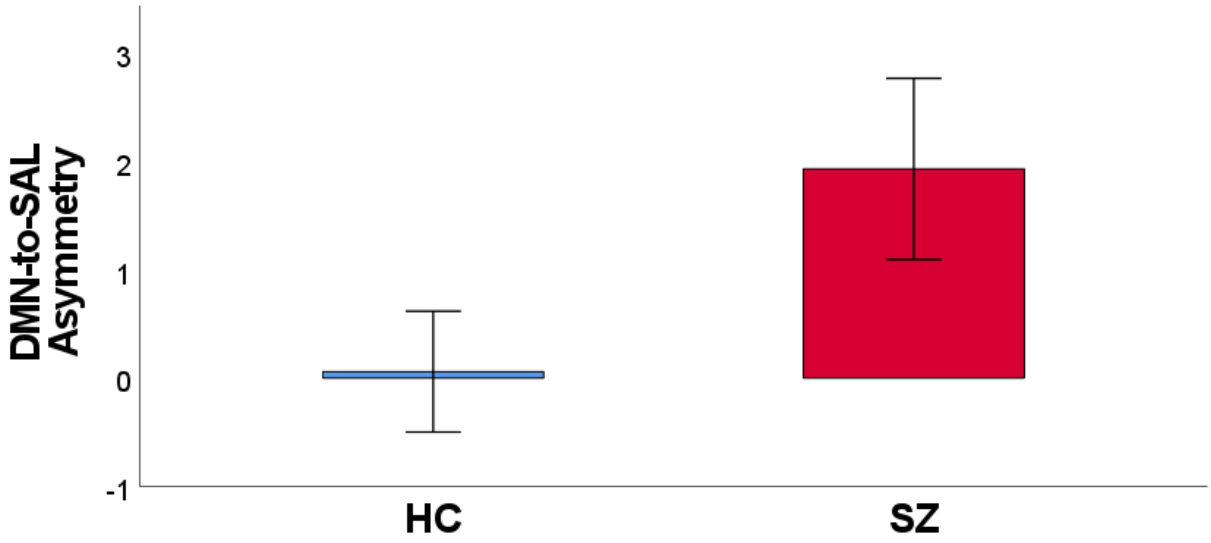

Figure 14. Group (SZ, HC) differences in Granger causality (GC) asymmetry between DMN and SAL using fMRI data. Greater GC was found from DMN to SAL than from SAL to DMN in SZ (red). HC (blue) do not demonstrate this GC asymmetry. Error bars denote +/- SE.

There was no main effect of DMN-SAL GC asymmetry on N100 amplitude to S1 *(β = 0.04, t(50)=0.3, p = 0.8*), nor was there an interaction between Group and DMN-SAL GC asymmetry (*β = 0.2, t(47)=1.0, p = 0.3)*. Similarly, DMN-SAL GC asymmetry did not predict the N100 ratio score ((*β =- 0.1, t(49) = 0.7, p = 0.5)* nor was there an interaction between Group and DMN-SAL GC asymmetry (*β = 0.3, t(47) = 0.1, p = 0.9)*.

Analyses examining possible mediation of the effect of Group on N100 variables by rs-fMRI-derived DMN-SAL GC asymmetry produced no reliable effects. Group status did not influence N100 amplitude to S1 *(-0.1, CI = -0.5 to 0.2*) or the N100 ratio score *(-0.03, CI = -0.2 to 0.08*) indirectly through resting state DMN-SAL GC.

Discussion

The goal of Study Aim 3 was to determine whether SZ demonstrate alterations in DMN-to-SAL directed connectivity and whether these alterations predict salience and inhibitory processing deficits indexed by N100 measures. As expected, SZ demonstrated greater resting state DMN-to-SAL effective connectivity than SAL-to-DMN connectivity, and HC showed no such asymmetry, such that DMN appears to be exerting outsized influence on SAL in SZ. The lack of effects on N100 variables, with no interactions or mediation effects, indicates that aberrant communication within this functional circuit is related to processes other than those indexed by N100. Contrary to hypotheses, no group differences in effective connectivity between DMN and SAL were identified in task-based EEG during the S1-S2 paradigm. Together, these findings suggest that SZ demonstrate alterations in intrinsic, task-independent DMN-SAL network communication. Not only did FE SZ show increased resting state intra-DMN connectivity relative to HC (see Study Aim 1), but DMN also appeared to exert more influence on SAL. In SZ, DMN and the self-referential processes it supports may be exerting excessive influence on SAL, thereby influencing what is judged as salient.

Contrary to hypotheses, resting state DMN-to-SAL effective connectivity did not predict either of the N100 variables included in the present study. Studies demonstrating similar dysfunction in the DMN-SAL circuit in SZ have related this pattern of abnormal directed connectivity to symptoms of psychosis, including hallucinations (Manoliu et al., 2014; Mallikarjun et al., 2018) and flat affect (Hare et al., 2019). Hare and colleagues (2019) also assessed network relationships with the attention subscale of the Scale for the Assessment of Negative Symptoms (SANS); this measure of attention was observed to be related only to intra-DMN connectivity and not DMN-SAL connectivity. In combination with findings from the present study and those from Study Aim 2, the mechanism supporting attentional processing

dysfunction in SZ via DMN may not involve directed relationships with SAL. Instead, dysfunction within the DMN-SAL circuit may support other positive and negative symptoms in the disorder. Planned follow-up assessment of the relationships between DMN-to-SAL effective connectivity and specific psychotic symptoms will aid in elucidation of the specific clinical impact of dysfunction in this neural circuit.

Although group differences were found in resting state DMN-SAL effective connectivity using fMRI, these differences were not replicated using EEG. This may be, in part, related to the difference in frequencies captured by each imaging modality. rs-fMRI connectivity captures very low-frequency fluctuations, between ~0.01-0.25 Hz (Gohel & Biswal, 2015), whereas the frequency band assessed in EEG oscillatory analyses for the present study was 2-40 Hz. Another possible explanation for the discrepancy between EEG and fMRI assessments of DMN-to-SAL effective connectivity is related to the processing of the data. Whereas connectivity analyses using EEG oscillatory data were computed on frequency-resolved EEG, the fMRI data used for connectivity analyses were the raw time series. Therefore, what was being compared in the present multimodal fusion analyses was not time-domain EEG vs. fMRI, but frequency-resolved EEG vs. time-domain fMRI. Thus, differences in the quantification of these two modalities may have influenced the variance in effective connectivity between networks captured with each measure.

Because no group differences were identified in the EEG-derived effective connectivity analyses, there were no clusters in time and frequency (see Study Aims 1 and 2) from which to extract each participant's average connectivity for use as a variable in multimodal data fusion analyses. To facilitate multimodal data fusion of EEG- and fMRI-derived DMN-to-SAL effective connectivity, possible follow-up analyses include averaging effective connectivity

across a priori frequency bands, such as those identified in Study Aims 1 and 2 (i.e., 4-7 Hz in the task data, 25-30 Hz in the rest data) or following general frequency band designations (e.g., delta, theta, alpha, beta).

In summary, the primary contribution of Study Aim 3 was demonstration of greater DMN-to-SAL directed connectivity in SZ than HC as assessed with resting state fMRI data. An implication of this finding is that salience processing in SZ may be biased towards the self-referential processes supported by DMN which, in turn, may correspond to features of the disorder.

General Discussion

Multimodal data from this dissertation reveal several important findings across the three study aims regarding disruptions to communications within and between the DMN and SAL networks in SZ that may contribute to cognitive impairments and symptoms in the disorder. Per Study Aim 1, this dissertation provides a novel replication and extension of resting state intra-DMN hyperconnectivity in a FE SZ sample using oscillatory EEG. A similar pattern of intrinsic DMN hyperconnectivity was also observed using fMRI data, demonstrating cross-modal replication. Although these measures of intrinsic DMN connectivity were correlated with one another, they also differed in their relationships with N100 ERP variables in SZ vs. HC. fMRI-derived DMN connectivity uniquely captured variance in the relationships between DMN connectivity, group (SZ, HC), and measures of N100 amplitude to S1 and N100 suppression. Present findings suggest that there are both shared and distinct signal components revealed by these neuroimaging methods in their sensitivity to intra-DMN connectivity. Despite differences across the two modalities, resting state hyperconnectivity of DMN was observed in both EEG- and fMRI-derived networks. This multimodal consistency in the present FE sample argues that

increased intrinsic connectivity within DMN represents a psychophysiological characteristic of SZ.

The extent to which DMN function supports not only internally-directed processing but externally-directed cognitive processing is not well understood. Much of the research literature suggests that DMN is a "task negative" network that becomes largely deactivated during the completion of tasks, though a small yet growing body of research indicates that engagement of DMN may actually support processing during tasks involving externally-oriented attention. Consistent with the larger body of research examining abnormal DMN function in SZ, it was hypothesized that SZ would demonstrate less suppression of DMN during a paired-stimulus paradigm. In fact, SZ exhibited less intra-DMN connectivity following S1 onset than HC. Thus, contrary to the conjecture of insufficient DMN suppression, SZ actually showed more suppression. Although DMN suppression during cognitive tasks has largely been viewed as beneficial, it is possible that preserved DMN function supports the attentional processes elicited by the task. Prevailing theories have posited that DMN plays a limited or purely detrimental role during externally-focused tasks, but present findings lend support to a nascent line of research suggesting that the role of DMN is much more complex and flexible. The anatomy of the DMN, including PFC and temporal regions, may be uniquely critical to the orientation of attention to auditory stimuli. In HC, increased connectivity within DMN following S1 may support global information integration during S1-S2 processing. Aberrant responsiveness of DMN during the paired-stimulus paradigm in SZ may represent a mechanism of dysfunction in these processes. Although this pattern of DMN connectivity during the task did not predict N100 abnormalities in SZ, it may predict other aspects of cognitive dysfunction.

In accordance with Study Aim 3, SZ were expected to exhibit greater directed connectivity from DMN to SAL such that salience processing in the disorder is biased towards DMN and the self-referential processes it supports. In line with this hypothesis, SZ demonstrated higher resting state DMN-to-SAL effective connectivity as assessed with fMRI. These results build upon the findings of resting state DMN hyperconnectivity in SZ, observed in Study Aim 1, and demonstrate that DMN also exerts greater influence on SAL in SZ. Given proposed functions of these networks, it appears that DMN is unduly influencing salience processing among SZ. Increased salience ascribed to processes related to self-awareness, in turn, may contribute to the presence of psychotic symptoms related to self-disturbance. Although this measure of directed connectivity between DMN and SAL networks did not predict either N100 variable in the present study, specific evaluation of relationships between DMN-to-SAL directed connectivity and positive symptoms of psychosis may clarify the role of abnormal connectivity within this circuit in SZ.

Two separate profiles of abnormal DMN connectivity in SZ were observed; hyperconnectivity observed in the resting state and hypoconnectivity observed during the paired-stimulus paradigm. These distinct profiles of abnormal DMN function suggest distinctly targeted interventions for different patients. DMN hyperconnectivity is thought to contribute to cognitive symptoms including paranoia and hallucinations (Rotarska-Jagiela et al., 2010). Among SZ exhibiting DMN resting state hyperconnectivity, interventions that aim to reduce this hyperconnectivity may contribute to reductions in these psychotic symptoms.

Mindfulness-based interventions have demonstrated promise in reducing DMN activity (Scheibner et al., 2017). Experienced meditators have similarly been found to exhibit weaker resting state intra-DMN connectivity than novice meditators (Taylor et al., 2014). Given present

findings of DMN hyperconnectivity in FE SZ and previous work demonstrating DMN hyperconnectivity even among unaffected siblings (Liu et al., 2012) and those at ultra-high risk for the development of psychosis **(**Shim et al., 2010**),** mindfulness training could potentially serve as an early intervention that reduces the risk of developing SZ via normalization of DMN hyperconnectivity. Relationships between mindfulness practice and activity in the DMN-SAL circuit have also been demonstrated (Hasenkamp et al., 2012; Masuda et al., 2010; Shaurya Prakash et al., 2013; Zeidan et al., 2011). Acceptance and Commitment Therapy, a third-wave cognitive behavioral therapy with a core emphasis on mindfulness, has been found to reduce connectivity within DMN as well as connectivity between DMN and SAL (Aytur et al., 2021). These findings suggest that mindfulness-based approaches may also benefit SZ exhibiting abnormalities in DMN-SAL effective connectivity. In addition to behavioral interventions, pharmaceutical interventions may be tailored to address DMN abnormalities in SZ. Ketamine, for example, has been shown to decrease functional connectivity within DMN via glutamatergic modulation (Li et al., 2018).

For patients specifically demonstrating hypoconnectivity or reduced task-activated DMN function, cognitive training (CT) may represent a promising intervention. Cao and colleagues (2016) found that provision of 24 sessions of CT over the course of 3 months was associated with increased functional connectivity within DMN as well as SAL and the central executive network. Given research demonstrating the ability of CT to improve cognitive deficits in SZ (von Bastian et al., 2022; Nuechterlein et al., 2014, 2016), it is possible that some of these improvements occur through modifications in DMN connectivity. Data for this dissertation came from SZ enrolled in a CT only or CT combined with exercise intervention. Although present findings were obtained from data collected in patients prior to starting either intervention, it

would be beneficial to evaluate these same participants after completion of the RCT to determine whether intervention-related improvements in cognitive or psychotic symptoms were associated with and perhaps mediated by alterations in DMN connectivity. In addition to CT, modified electroconvulsive therapy applied to SZ has been found to increase global functional connectivity density within DMN in SZ (Huang et al., 2018). Such an intervention could similarly serve to normalize deficits in DMN connectivity.

This dissertation is innovative in its effort to link two typically disparate bodies of research, fMRI and EEG/ERP, in order to characterize the mechanism associated with aberrant salience monitoring and inhibitory dysfunction in SZ. Integrating information across modalities -- specifically, oscillatory EEG, resting state EEG, and resting state fMRI -- decreases the influence of method variance and improves our ability to operationalize psychological constructs (Cronbach & Meehl, 1955; Kozak & Miller, 1982; Miller et al., 2016; Patrick & Bernat, 2010). Furthermore, this dissertation drew from the fMRI literature to define neural networks and applied current understanding of these networks to guide analysis of high-temporal-resolution, source-localized EEG oscillatory and ERP data collected during a paired-stimulus paradigm. In turn, established N100 abnormalities of SZ informed the hypotheses and analytic approaches regarding abnormal information processing and salience monitoring that were examined in resting state fMRI. Thus, employing EEG and fMRI methods was intended to improve the ability to identify psychophysiological mechanisms of abnormality in schizophrenia.

In conclusion, results presented here demonstrate specific profiles of DMN function in FE SZ that differentially relate to attentional processes indexed by measures obtained from the N100 ERP component. It was hypothesized that abnormalities in DMN and SAL network function and N100 variables would capture dysfunction within shared mechanisms. Results revealed

relationships between these neural network and ERP measures, though they also identified unique alterations within measures that may predict particular cognitive deficits. Future work can build upon this research to further clarify how alterations in these neural mechanisms contribute to vulnerability to and maintenance of disorder-related impairments and inform promising targets for effective prevention and treatment interventions.

References

Andreou, C., Leicht, G., Nolte, G., Polomac, N., Moritz, S., Karow, A., ... & Mulert, C. (2015). Resting-state theta-band connectivity and verbal memory in schizophrenia and in the high-risk state. Schizophrenia research, 161(2-3), 299-307.

Anticevic, A., Cole, M. W., Murray, J. D., Corlett, P. R., Wang, X. J., & Krystal, J. H. (2012). The role of default network deactivation in cognition and disease. In *Trends in Cognitive Sciences*. https://doi.org/10.1016/j.tics.2012.10.008

Anticevic, A., Repovs, G., Shulman, G. L., & Barch, D. M. (2010). When less is more: TPJ and default network deactivation during encoding predicts working memory performance. *NeuroImage*. https://doi.org/10.1016/j.neuroimage.2009.11.008

Astolfi, L., De Vico Fallani, F., Cincotti, F., Mattia, D., Marciani, M. G., Bufalari, S., Salinari, S., Colosimo, A., Ding, L., Edgar, J. C., Heller, W., Miller, G. A., He, B., & Babiloni, F. (2007). Imaging functional brain connectivity patterns from high-resolution EEG and fMRI via graph theory. *Psychophysiology*, *44*(6), 880–893. https://doi.org/10.1111/j.1469-8986.2007.00556.x

Aytur, S. A., Ray, K. L., Meier, S. K., Campbell, J., Gendron, B., Waller, N., & Robin, D. A. (2021). Neural mechanisms of acceptance and commitment therapy for chronic pain: A network-based fMRI approach. Frontiers in human neuroscience, 15, 28.

Baenninger, A., Palzes, V. A., Roach, B. J., Mathalon, D. H., Ford, J. M., & Koenig, T. (2017). Abnormal Coupling between Default Mode Network and Delta and Beta Band Brain Electric Activity in Psychotic Patients. *Brain Connectivity*. https://doi.org/10.1089/brain.2016.0456

Bakhshayesh, H., Fitzgibbon, S. P., Janani, A. S., Grummett, T. S., & Pope, K. J. (2019). Detecting synchrony in EEG: A comparative study of functional connectivity measures. *Computers in Biology and Medicine*. https://doi.org/10.1016/j.compbiomed.2018.12.005

Barnett, L., Barrett, A. B., & Seth, A. K. (2009). Granger causality and transfer entropy Are equivalent for gaussian variables. *Physical Review Letters*. https://doi.org/10.1103/PhysRevLett.103.238701

Bell, M. A., & Cuevas, K. (2012). Using EEG to Study Cognitive Development: Issues and Practices. In *Journal of Cognition and Development*. https://doi.org/10.1080/15248372.2012.691143

Berger, H. (1929). Uber das Elektrenkephalogrammdes Menschen. Archiv fur Psychiatrie m d Nervenkrankheiten. 87, 527-570

Berger, H. (I 930). Uber das Elekfrenkephalograrnmdes Menschen. Zweite Mitteilung. Journal of Psychology and Neurology. 40, 160-179

Bidet-Caulet, A., Mikyska, C., & Knight, R. T. (2010). Load effects in auditory selective attention: Evidence for distinct facilitation and inhibition mechanisms. *NeuroImage*. https://doi.org/10.1016/j.neuroimage.2009.12.039

Bonnelle, V., Ham, T. E., Leech, R., Kinnunen, K. M., Mehta, M. A., Greenwood, R. J., & Sharp, D. J. (2012). Salience network integrity predicts default mode network function after traumatic brain injury. *Proceedings of the National Academy of Sciences of the United States of America*. https://doi.org/10.1073/pnas.1113455109

Boutros, N. N., & Belger, A. (1999). Midlatency evoked potentials attenuation and augmentation reflect different aspects of sensory gating. In *Biological Psychiatry*. https://doi.org/10.1016/S0006-3223(98)00253-4

Boutros, N. N., Korzyukov, O., Jansen, B., Feingold, A., & Bell, M. (2004). Sensory gating deficits during the mid-latency phase of information processing in medicated schizophrenia patients. *Psychiatry Research*. https://doi.org/10.1016/j.psychres.2004.01.007

Boutros, N. N., Brockhaus-Dumke, A., Gjini, K., Vedeniapin, A., Elfakhani, M., Burroughs, S., Keshavan, M. (2009). Sensory-gating deficit of the N100 mid-latency auditory evoked potential in medicated schizophrenia patients. *Schizophrenia Research.* https://doi.org/10.1016/j.schres.2009.05.019

Bowie, C. R., & Harvey, P. D. (2006). Cognitive deficits and functional outcome in schizophrenia. In *Neuropsychiatric Disease and Treatment*. https://doi.org/10.2147/nedt.2006.2.4.531

Bowman, A. D., Griffis, J. C., Visscher, K. M., Dobbins, A. C., Gawne, T. J., DiFrancesco, M. W., & Szaflarski, J. P. (2017). Relationship between alpha rhythm and the default mode network: an EEG-fMRI study. Journal of clinical neurophysiology: official publication of the American Electroencephalographic Society, 34(6), 527.

Braga, R. M., Sharp, D. J., Leeson, C., Wise, R. J., & Leech, R. (2013). Echoes of the brain within default mode, association, and heteromodal cortices. Journal of Neuroscience, 33(35), 14031-14039.

Bramon, E., Rabe-Hesketh, S., Sham, P., Murray, R. M., & Frangou, S. (2004). Meta-analysis of the P300 and P50 waveforms in schizophrenia. *Schizophrenia Research*. https://doi.org/10.1016/j.schres.2004.01.004

Bressler, S. L., Tang, W., Sylvester, C. M., Shulman, G. L., & Corbetta, M. (2008). Top-down control of human visual cortex by frontal and parietal cortex in anticipatory visual spatial attention. *J Neurosci*. https://doi.org/10.1523/JNEUROSCI.1776-08.2008

Brockhaus-Dumke, A., Schultze-Lutter, F., Mueller, R., Tendolkar, I., Bechdolf, A., Pukrop, R., Klosterkoetter, J., & Ruhrmann, S. (2008). Sensory Gating in Schizophrenia: P50 and N100 Gating in Antipsychotic-Free Subjects at Risk, First-Episode, and Chronic Patients. *Biological Psychiatry*. https://doi.org/10.1016/j.biopsych.2008.02.006

Brookes, M. J., O'Neill, G. C., Hall, E. L., Woolrich, M. W., Baker, A., Palazzo Corner, S., Robson, S. E., Morris, P. G., & Barnes, G. R. (2014). Measuring temporal, spectral and spatial changes in electrophysiological brain network connectivity. *NeuroImage*. https://doi.org/10.1016/j.neuroimage.2013.12.066

Buckner, R. L., Andrews-Hanna, J. R., & Schacter, D. L. (2008). The brain's default network: Anatomy, function, and relevance to disease. In *Annals of the New York Academy of Sciences*. https://doi.org/10.1196/annals.1440.011

Cavanagh, J. F., & Frank, M. J. (2014). Frontal theta as a mechanism for cognitive control. Trends in cognitive sciences, 18(8), 414-421.

Chadick, J. Z., & Gazzaley, A. (2011). Differential coupling of visual cortex with default or frontal-parietal network based on goals. *Nature Neuroscience*. https://doi.org/10.1038/nn.2823

Chang, C., & Glover, G. H. (2010). Time-frequency dynamics of resting state brain connectivity measured with fMRI. *NeuroImage*. https://doi.org/10.1016/j.neuroimage.2009.12.011

Connolly, J. F., Manchanda, R., Gruzelier, J. H., & Hirsch, S. R. (1985). Pathway and hemispheric differences in the event-related potential (ERP) to monaural stimulation: A comparison of schizophrenic patients with normal controls. *Biological Psychiatry*. https://doi.org/10.1016/0006-3223(85)90059-9

Cronbach, L. J., & Meehl, P. E. (1955). Construct validity in psychological tests. *Psychological*

Bulletin. https://doi.org/10.1037/h0040957

De Vries, R., Heeringc, H. D., Postmes, L., Goedhart, S., Sno, H. N., & de Lieuwe, H. (2013). Self-disturbance in schizophrenia: A phenomenological approach to better understand our patients. *Primary Care Companion to the Journal of Clinical Psychiatry*. https://doi.org/10.4088/PCC.12m01382

Dosenbach, N. U. F., Fair, D. A., Miezin, F. M., Cohen, A. L., Wenger, K. K., Dosenbach, R. A. T., Fox, M. D., Snyder, A. Z., Vincent, J. L., Raichle, M. E., Schlaggar, B. L., & Petersen, S. E. (2007). Distinct brain networks for adaptive and stable task control in humans. *Proceedings of the National Academy of Sciences of the United States of America*. https://doi.org/10.1073/pnas.0704320104

Engel, A. K., & Fries, P. (2010). Beta-band oscillations—signalling the status quo?. Current opinion in neurobiology, 20(2), 156-165.

Fan, F., Tan, Y., Wang, Z., Yang, F., Fan, H., Xiang, H., Guo, H., Hong, L. E., Tan, S., & Zuo, X.-N. (2019). Functional fractionation of default mode network in first episode schizophrenia. *Schizophrenia Research*, *210*, 115–121. https://doi.org/10.1016/J.SCHRES.2019.05.038

Ford, J. M., & Mathalon, D. H. (2005). Corollary discharge dysfunction in schizophrenia: Can it explain auditory hallucinations? *International Journal of Psychophysiology*. https://doi.org/10.1016/j.ijpsycho.2005.01.014

Freedman, R., Adler, L. E., Gerhardt, G. A., Waldo, M., Baker, N., Rose, G. M., Drebing, C., Nagamoto, H., Bickford-Wimer, P., & Franks, R. (1987). Neurobiological studies of sensory gating in schizophrenia. *Schizophrenia Bulletin*. https://doi.org/10.1093/schbul/13.4.669

Fryer, S. L., Woods, S. W., Kiehl, K. A., Calhoun, V. D., Pearlson, G. D., Roach, B. J., Ford, J. M., Srihari, V. H., McGlashan, T. H., & Mathalon, D. H. (2013). Deficient suppression of default mode regions during working memory in individuals with early psychosis and at clinical high-risk for psychosis. *Frontiers in Psychiatry*. https://doi.org/10.3389/fpsyt.2013.00092

Galindo, L., Bergé, D., Murray, G. K., Mané, A., Bulbena, A., Perez, V., & Vilarroya, O. (2018). Default mode network aberrant connectivity associated with neurological soft signs in schizophrenia patients and unaffected relatives. Frontiers in Psychiatry, 8, 298.

Garrity, A. G., Pearlson, G. D., McKiernan, K., Lloyd, D., Kiehl, K. A., & Calhoun, V. D. (2007). Aberrant "default mode" functional connectivity in schizophrenia. *American Journal of Psychiatry*. https://doi.org/10.1176/ajp.2007.164.3.450

Geweke, J. (1982). Measurement of linear dependence and feedback between multiple time series. Journal of the American statistical association, 77(378), 304-313.

Gjini, K., Burroughs, S., & Boutros, N. N. (2011). Relevance of attention in auditory sensory gating paradigms in schizophrenia: A pilot study. *Journal of Psychophysiology*. https://doi.org/10.1027/0269-8803/a000042

Goerg, G. M. (2015). The lambert way to gaussianize heavy-tailed data with the inverse of Tukey's h transformation as a special case. The Scientific World Journal, 2015.

Gold, J. M., Robinson, B., Leonard, C. J., Hahn, B., Chen, S., McMahon, R. P., & Luck, S. J. (2018). Selective attention, working memory, and executive function as potential independent sources of cognitive dysfunction in schizophrenia. *Schizophrenia Bulletin*. https://doi.org/10.1093/schbul/sbx155

Granger, C. W. J. (1969). Investigating Causal Relations by Econometric Models and Cross-

spectral Methods. *Econometrica*, *37*(3), 424. https://doi.org/10.2307/1912791

Greicius, M. D., Krasnow, B., Reiss, A. L., & Menon, V. (2003). Functional connectivity in the resting brain: A network analysis of the default mode hypothesis. *Proceedings of the National Academy of Sciences of the United States of America*. https://doi.org/10.1073/pnas.0135058100

Guha, A., Brier, M. R., Ortega, M., Westerhaus, E., Nelson, B., & Ances, B. M. (2016). Topographies of cortical and Subcortical volume loss in HIV and aging in the cART Era. *Journal of Acquired Immune Deficiency Syndromes*. https://doi.org/10.1097/QAI.0000000000001111

Guha, A., Wang, L., Tanenbaum, A., Esmaeili-Firidouni, P., Wendelken, L. A., Busovaca, E., Clifford, K., Desai, A., Ances, B. M., & Valcour, V. (n.d.). *Intrinsic network connectivity abnormalities in HIV-infected individuals over age 60*. https://doi.org/10.1007/s13365-015-0370-y

Guo, W., Liu, F., Chen, J., Wu, R., Li, L., Zhang, Z., Chen, H., & Zhao, J. (2017). Hyperactivity of the default-mode network in first-episode, drug-naive schizophrenia at rest revealed by family-based case-control and traditional case-control designs. *Medicine (United States)*. https://doi.org/10.1097/MD.0000000000006223

Ham, T., Leff, A., de Boissezon, X., Joffe, A., & Sharp, D. J. (2013). Cognitive control and the salience network: An investigation of error processing and effective connectivity. *Journal of Neuroscience*. https://doi.org/10.1523/JNEUROSCI.4692-12.2013

Hare, S. M., Ford, J. M., Mathalon, D. H., Damaraju, E., Bustillo, J., Belger, A., Lee, H. J., Mueller, B. A., Lim, K. O., Brown, G. G., Preda, A., van Erp, T. G. M., Potkin, S. G., Calhoun, V. D., & Turner, J. A. (2019). Salience–Default Mode Functional Network

Connectivity Linked to Positive and Negative Symptoms of Schizophrenia. *Schizophrenia Bulletin*. https://doi.org/10.1093/schbul/sby112

Hasenkamp, W., Wilson-Mendenhall, C. D., Duncan, E., & Barsalou, L. W. (2012). Mind wandering and attention during focused meditation: A fine-grained temporal analysis of fluctuating cognitive states. NeuroImage, 59(1), 750–760. https://doi.org/10.1016/j.neuroimage.2011.07.008

Hayes, A. F. (2012). PROCESS: A versatile computational tool for observed variable mediation, moderation, and conditional process modeling.

Hayes, A. F. (2017). Introduction to mediation, moderation, and conditional process analysis: A regression-based approach. Guilford publications.

Howes, O. D., & Murray, R. M. (2014). Schizophrenia: An integrated sociodevelopmental-cognitive model. In *The Lancet*. https://doi.org/10.1016/S0140-6736(13)62036-X

Hsieh, M. H., Shan, J. C., Huang, W. L., Cheng, W. C., Chiu, M. J., Jaw, F. S., ... & Liu, C. C. (2012). Auditory event-related potential of subjects with suspected pre-psychotic state and first-episode psychosis. Schizophrenia research, 140(1-3), 243-249.

Hu, M. L., Zong, X. F., Mann, J. J., Zheng, J. J., Liao, Y. H., Li, Z. C., He, Y., Chen, X. G., & Tang, J. S. (2017). A Review of the Functional and Anatomical Default Mode Network in Schizophrenia. In *Neuroscience Bulletin*. https://doi.org/10.1007/s12264-016-0090-1

Huang, H., Jiang, Y., Xia, M., Tang, Y., Zhang, T., Cui, H., ... & Wang, J. (2018). Increased resting state global functional connectivity density of default mode network in schizophrenia subjects treated with electroconvulsive therapy. Schizophrenia research, 197, 192-199.

Jafri, M. J., Pearlson, G. D., Stevens, M., & Calhoun, V. D. (2008). A method for functional

network connectivity among spatially independent resting state components in schizophrenia. *NeuroImage*. https://doi.org/10.1016/j.neuroimage.2007.11.001

Jann, K., Dierks, T., Boesch, C., Kottlow, M., Strik, W., & Koenig, T. (2009). BOLD correlates of EEG alpha phase-locking and the fMRI default mode network. *NeuroImage*. https://doi.org/10.1016/j.neuroimage.2009.01.001

Javitt, D. C., & Freedman, R. (2015). Sensory processing dysfunction in the personal experience and neuronal machinery of schizophrenia. *American Journal of Psychiatry*. https://doi.org/10.1176/appi.ajp.2014.13121691

Keil, A., Debener, S., Gratton, G., Junghöfer, M., Kappenman, E. S., Luck, S. J., Luu, P., Miller, G. A., & Yee, C. M. (2014). Committee report: Publication guidelines and recommendations for studies using electroencephalography and magnetoencephalography. *Psychophysiology*. https://doi.org/10.1111/psyp.12147

Keller, A. S., Payne, L., & Sekuler, R. (2017). Characterizing the roles of alpha and theta oscillations in multisensory attention. Neuropsychologia, 99, 48-63.

Kindler, J., Jann, K., Homan, P., Hauf, M., Walther, S., Strik, W., ... & Hubl, D. (2015). Static and dynamic characteristics of cerebral blood flow during the resting state in schizophrenia. Schizophrenia bulletin, 41(1), 163-170.

Klimesch, W., Doppelmayr, M., Schimke, H., & Ripper, B. (1997). Theta synchronization and alpha desynchronization in a memory task. Psychophysiology, 34(2), 169-176.

Knyazev, G. G., Slobodskoj-Plusnin, J. Y., Bocharov, A. V., & Pylkova, L. V. (2011). The default mode network and EEG alpha oscillations: An independent component analysis. *Brain Research*. https://doi.org/10.1016/j.brainres.2011.05.052

Kopp, B., Mattler, U., & Rist, F. (1994). Selective attention and response competition in

schizophrenic patients. *Psychiatry Research*. https://doi.org/10.1016/0165-1781(94)90104-X

Kozak, M. J., & Miller, G. a. (1982). Hypothetical constructs versus intervening variables: A re-appraisal of the three-systems model of anxiety assessment. *Behavioral Assessment*.

Krukow, P., Jonak, K., Grochowski, C., Plechawska-Wójcik, M., & Karakuła-Juchnowicz, H. (2020). Resting-state hyperconnectivity within the default mode network impedes the ability to initiate cognitive performance in first-episode schizophrenia patients. Progress in Neuro-Psychopharmacology and Biological Psychiatry, 102, 109959.

Laird, A. R., Lancaster, J. J., & Fox, P. T. (2005). Brainmap. Neuroinformatics, 3(1), 65-77.

Laufs, H., Krakow, K., Sterzer, P., Eger, E., Beyerle, A., Salek-Haddadi, A., & Kleinschmidt, A. (2003). Electroencephalographic signatures of attentional and cognitive default modes in spontaneous brain activity fluctuations at rest. Proceedings of the national academy of sciences, 100(19), 11053-11058.

Lee, T. H., Kim, M., Hwang, W. J., Kim, T., Kwak, Y. Bin, & Kwon, J. S. (2019). Relationship between resting state theta phase-gamma amplitude coupling and neurocognitive functioning in patients with first-episode psychosis. *Schizophrenia Research*, *xxxx*. https://doi.org/10.1016/j.schres.2019.12.010

Li, M., Woelfer, M., Colic, L., Safron, A., Chang, C., Heinze, H. J., ... & Walter, M. (2020). Default mode network connectivity change corresponds to ketamine's delayed glutamatergic effects. European archives of psychiatry and clinical neuroscience, 270(2), 207-216.

Lijffijt, M., Lane, S. D., Meier, S. L., Boutros, N. N., Burroughs, S., Steinberg, J. L., Gerard Moeller, F., & Swann, A. C. (2009). P50, N100, and P200 sensory gating: Relationships

with behavioral inhibition, attention, and working memory. *Psychophysiology*. https://doi.org/10.1111/j.1469-8986.2009.00845.x

Liu, H., Kaneko, Y., Ouyang, X., Li, L., Hao, Y., Chen, E. Y. H., Jiang, T., Zhou, Y., & Liu, Z. (2012). Schizophrenic patients and their unaffected siblings share increased resting state connectivity in the task-negative network but not its anticorrelated task-positive network. *Schizophrenia Bulletin*. https://doi.org/10.1093/schbul/sbq074

Liu, Q., Farahibozorg, S., Porcaro, C., Wenderoth, N., & Mantini, D. (2017). Detecting large-scale networks in the human brain using high-density electroencephalography. *Human Brain Mapping*. https://doi.org/10.1002/hbm.23688

Luck, S. J., Leonard, C. J., Hahn, B., & Gold, J. M. (2019). Is Attentional Filtering Impaired in Schizophrenia? *Schizophrenia Bulletin*. https://doi.org/10.1093/schbul/sbz045

Luo, Q., Ge, T., Grabenhorst, F., Feng, J., & Rolls, E. T. (2013). Attention-Dependent Modulation of Cortical Taste Circuits Revealed by Granger Causality with Signal-Dependent Noise. *PLoS Computational Biology*. https://doi.org/10.1371/journal.pcbi.1003265

Mallikarjun, P. K., Lalousis, P. A., Dunne, T. F., Heinze, K., Reniers, R. L., Broome, M. R., Farmah, B., Oyebode, F., Wood, S. J., & Upthegrove, R. (2018). Aberrant salience network functional connectivity in auditory verbal hallucinations: A first episode psychosis sample. *Translational Psychiatry*. https://doi.org/10.1038/s41398-018-0118-6

Manoliu, A., Riedl, V., Zherdin, A., Mühlau, M., Schwerthöffer, D., Scherr, M., Peters, H., Zimmer, C., Förstl, H., Bäuml, J., Wohlschläger, A. M., & Sorg, C. (2014). Aberrant Dependence of Default Mode/Central Executive Network Interactions on Anterior Insular Salience Network Activity in Schizophrenia. *Schizophrenia Bulletin*, *40*(2), 428–437.

https://doi.org/10.1093/schbul/sbt037

Maris, E., & Oostenveld, R. (2007). Nonparametric statistical testing of EEG- and MEG-data. *Journal of Neuroscience Methods*. https://doi.org/10.1016/j.jneumeth.2007.03.024

Masuda, A., Twohig, M. P., Stormo, A. R., Feinstein, A. B., Chou, Y. Y., & Wendell, J. W. (2010). The effects of cognitive defusion and thought distraction on emotional discomfort and believability of negative self-referential thoughts. Journal of Behavior Therapy and Experimental Psychiatry, 41(1), 11–17. https://doi.org/10.1016/j.jbtep.2009.08.006

Menon, V. (2015). Salience Network. In *Brain Mapping: An Encyclopedic Reference*. https://doi.org/10.1016/B978-0-12-397025-1.00052-X

Menon, Vinod. (2011). Large-scale brain networks and psychopathology: A unifying triple network model. In *Trends in Cognitive Sciences*. https://doi.org/10.1016/j.tics.2011.08.003

Menon, Vinod, & Uddin, L. Q. (2010). Saliency, switching, attention and control: a network model of insula function. In *Brain structure & function*. https://doi.org/10.1007/s00429-010-0262-0

Michel, C. M., & He, B. (2019). EEG source localization. In *Handbook of Clinical Neurology*. https://doi.org/10.1016/B978-0-444-64032-1.00006-0

Miller, G. A., Lutzenberger, W., & Elbert, T. (1991). The linked-reference issue in EEG and ERP recording. *Journal of Psychophysiology*.

Miller, G. A., & Rockstroh, B. S. (2016). Progress and Prospects for Endophenotypes for Schizophrenia in the Time of Genomics, Epigenetics, Oscillatory Brain Dynamics, and the Research Domain Criteria. In *The Neurobiology of Schizophrenia*. https://doi.org/10.1016/B978-0-12-801829-3.00010-0

Miller, Gregory A., Rockstroh, B. S., Hamilton, H. K., & Yee, C. M. (2016). Psychophysiology

as a core strategy in RDoC. *Psychophysiology*. https://doi.org/10.1111/psyp.12581

Nakhnikian, A., Oribe, N., Hirano, S., Hirano, Y., Levin, M., & Spencer, K. (2021). Increased Theta/Alpha Source Activity and Default Mode Network Connectivity in Schizophrenia During Eyes-Closed Rest. Biological Psychiatry, 89(9), S150-S151.

Nelson, B., Whitford, T. J., Lavoie, S., & Sass, L. A. (2014a). What are the neurocognitive correlates of basic self-disturbance in schizophrenia?: Integrating phenomenology and neurocognition. Part 1 (Source monitoring deficits). *Schizophrenia Research*. https://doi.org/10.1016/j.schres.2013.06.022

Nelson, B., Whitford, T. J., Lavoie, S., & Sass, L. A. (2014b). What are the neurocognitive correlates of basic self-disturbance in schizophrenia?: Integrating phenomenology and neurocognition. Part 2 (Aberrant salience). *Schizophrenia Research*. https://doi.org/10.1016/j.schres.2013.06.033

Nelson, B., Parnas, J., & Sass, L. A. (2014c). Disturbance of minimal self (ipseity) in schizophrenia: clarification and current status. Schizophrenia bulletin, 40(3), 479-482.

Neuner, I., Arrubla, J., Werner, C. J., Hitz, K., Boers, F., Kawohl, W., & Shah, N. J. (2014). The default mode network and EEG regional spectral power: a simultaneous fMRI-EEG study. PLoS One, 9(2), e88214.

Newson, J. J., & Thiagarajan, T. C. (2019). EEG Frequency Bands in Psychiatric Disorders: A Review of Resting State Studies. *Frontiers in Human Neuroscience*. https://doi.org/10.3389/fnhum.2018.00521

Nolte, G., Bai, O., Wheaton, L., Mari, Z., Vorbach, S., & Hallett, M. (2004). Identifying true brain interaction from EEG data using the imaginary part of coherency. *Clinical Neurophysiology*. https://doi.org/10.1016/j.clinph.2004.04.029

Nuechterlein, K. H., Ventura, J., Subotnik, K. L., Hayata, J. N., Medalia, A., & Bell, M. D. (2014). Developing a cognitive training strategy for first-episode schizophrenia: integrating bottom-up and top-down approaches. American journal of psychiatric rehabilitation, 17(3), 225-253.

Nuechterlein, K. H., Ventura, J., McEwen, S. C., Gretchen-Doorly, D., Vinogradov, S., & Subotnik, K. L. (2016). Enhancing cognitive training through aerobic exercise after a first schizophrenia episode: theoretical conception and pilot study. Schizophrenia bulletin, 42(suppl_1), S44-S52.

Northoff, G., Heinzel, A., De Greck, M., Bermpohl, F., Dobrowolny, H., & Panksepp, J. (2006). Self-referential processing in our brain—a meta-analysis of imaging studies on the self. Neuroimage, 31(1), 440-457.

O'Neill, A., Mechelli, A., & Bhattacharyya, S. (2019). Dysconnectivity of large-scale functional networks in early psychosis: A meta-analysis. *Schizophrenia Bulletin*. https://doi.org/10.1093/schbul/sby094

Orliac, F., Naveau, M., Joliot, M., Delcroix, N., Razafimandimby, A., Brazo, P., Dollfus, S., & Delamillieure, P. (2013). Links among resting state default-mode network, salience network, and symptomatology in schizophrenia. *Schizophrenia Research*. https://doi.org/10.1016/j.schres.2013.05.007

Palaniyappan, L., & Liddle, P. F. (2012). Does the salience network play a cardinal role in psychosis? An emerging hypothesis of insular dysfunction. In *Journal of Psychiatry and Neuroscience*. https://doi.org/10.1503/jpn.100176

Patriat, R., Molloy, E. K., Meier, T. B., Kirk, G. R., Nair, V. A., Meyerand, M. E., ... & Birn, R. M. (2013). The effect of resting condition on resting-state fMRI reliability and consistency:

a comparison between resting with eyes open, closed, and fixated. Neuroimage, 78, 463-473.

Patrick, C. J., & Bernat, E. M. (2010). Neuroscientific foundations of psychopathology. *Contemporary Directions in Psychopathology: Scientific Foundations of the DSM-V and ICD-11. BT - Contemporary Directions in Psychopathology: Scientific Foundations of the DSM-V and ICD-11.* https://doi.org/Cited By (since 1996) 8\rExport Date 8 May 2012

Patterson, J. V., Hetrick, W. P., Boutros, N. N., Jin, Y., Sandman, C., Stern, H., Potkin, S., & Bunney, W. E. (2008). P50 sensory gating ratios in schizophrenics and controls: A review and data analysis. *Psychiatry Research*. https://doi.org/10.1016/j.psychres.2007.02.009

Popov, T., Popova, P., Harkotte, M., Awiszus, B., Rockstroh, B., & Miller, G. A. (2018a). Cross-frequency interactions between frontal theta and posterior alpha control mechanisms foster working memory. NeuroImage, 181, 728-733.

Popov, T., Westner, B.U., Silton, R.L., Sass, S.M., Spielberg, J.M., Rockstroh, B., Heller, W., & Miller, G.A. (2018b). Time course of brain network reconfiguration supporting inhibitory control. Journal of Neuroscience, 38, 4348-4356. https://doi.org/10.1523/JNEUROSCI.2639-17.2018. PMCID: PMC5932643.

Potter, D., Summerfelt, A., Gold, J., & Buchanan, R. W. (2006). Review of clinical correlates of P50 sensory gating abnormalities in patients with schizophrenia. *Schizophrenia Bulletin*. https://doi.org/10.1093/schbul/sbj050

Power, J. D., Cohen, A. L., Nelson, S. M., Wig, G. S., Barnes, K. A., Church, J. A., Vogel, A. C., Laumann, T. O., Miezin, F. M., Schlaggar, B. L., & Petersen, S. E. (2011). Functional network organization of the human brain. *Neuron*, *72*(4), 665–678. https://doi.org/10.1016/j.neuron.2011.09.006

Power, J. D., Mitra, A., Laumann, T. O., Snyder, A. Z., Schlaggar, B. L., & Petersen, S. E. (2014). Methods to detect, characterize, and remove motion artifact in resting state fMRI. *NeuroImage*, *84*, 320–341. https://doi.org/10.1016/j.neuroimage.2013.08.048

Pruim, R. H. R., Mennes, M., van Rooij, D., Llera, A., Buitelaar, J. K., & Beckmann, C. F. (2015). ICA-AROMA: A robust ICA-based strategy for removing motion artifacts from fMRI data. *NeuroImage*. https://doi.org/10.1016/j.neuroimage.2015.02.064

Putcha, D., Ross, R. S., Cronin-Golomb, A., Janes, A. C., & Stern, C. E. (2016). Salience and default mode network coupling predicts cognition in aging and Parkinson's disease. *Journal of the International Neuropsychological Society*. https://doi.org/10.1017/S1355617715000892

Raichle, M. E. (2015). The Brain's Default Mode Network. *Annual Review of Neuroscience*. https://doi.org/10.1146/annurev-neuro-071013-014030

Roebroeck, A., Formisano, E., & Goebel, R. (2005). Mapping directed influence over the brain using Granger causality and fMRI. *NeuroImage*. https://doi.org/10.1016/j.neuroimage.2004.11.017

Rosburg, T. (2018). Auditory N100 gating in patients with schizophrenia: A systematic meta-analysis. *Clinical Neurophysiology*. https://doi.org/10.1016/j.clinph.2018.07.012

Rotarska-Jagiela, A., van de Ven, V., Oertel-Knöchel, V., Uhlhaas, P. J., Vogeley, K., & Linden, D. E. J. (2010). Resting-state functional network correlates of psychotic symptoms in schizophrenia. *Schizophrenia Research*. https://doi.org/10.1016/j.schres.2010.01.001

Roth, W. T., Goodale, J., & Pfefferbaum, A. (1991). Auditory event-related potentials and electrodermal activity in medicated and unmedicated schizophrenics. *Biological Psychiatry*. https://doi.org/10.1016/0006-3223(91)90094-3

Roth, W. T., Horvath, T. B., Pfefferbaum, A., & Kopell, B. S. (1980). Event-related potentials in schizophrenics. *Electroencephalography and Clinical Neurophysiology*. https://doi.org/10.1016/0013-4694(80)90299-0

Saletu, B., Itil, T. M., & Saletu, M. (1971). Auditory evoked response, EEG, and thought process in schizophrenics. *The American Journal of Psychiatry*. https://doi.org/10.1176/ajp.128.3.336

Sawaki, R., Kreither, J., Leonard, C. J., Kaiser, S. T., Hahn, B., Gold, J. M., & Luck, S. J. (2017). Hyperfocusing of attention on goal-related information in schizophrenia: Evidence from electrophysiology. *Journal of Abnormal Psychology*. https://doi.org/10.1037/abn0000209

Seeley, W. W. (2019). The salience network: a neural system for perceiving and responding to homeostatic demands. Journal of Neuroscience, 39(50), 9878-9882.

Seth, A. K., Barrett, A. B., & Barnett, L. (2015). Granger causality analysis in neuroscience and neuroimaging. *The Journal of Neuroscience : The Official Journal of the Society for Neuroscience*, *35*(8), 3293–3297. https://doi.org/10.1523/JNEUROSCI.4399-14.2015

Shagass, C., Roemer, R. A., Straumanis, J. J., & Amadeo, M. (1978). Evoked potential correlates of psychosis. *Biological Psychiatry*.

Shaurya Prakash, R., De Leon, A. A., Klatt, M., Malarkey, W., & Patterson, B. (2013). Mindfulness disposition and default-mode network connectivity in older adults. Social Cognitive and Affective Neuroscience, 8(1), 112–117. https://doi.org/10.1093/scan/nss115

Shim, G., Oh, J. S., Jung, W. H., Jang, J. H., Choi, C. H., Kim, E., Park, H. Y., Choi, J. S., Jung, M. H., & Kwon, J. S. (2010). Altered resting state connectivity in subjects at ultra-high risk for psychosis: An fMRI study. *Behavioral and Brain Functions*.

https://doi.org/10.1186/1744-9081-6-58

Smith, A. K., Edgar, J. C., Huang, M., Lu, B. Y., Thoma, R. J., Hanlon, F. M., McHaffie, G., Jones, A. P., Paz, R. D., Miller, G. A., & Cañive, J. M. (2010). Cognitive abilities and 50- and 100-msec paired-click processes in schizophrenia. *American Journal of Psychiatry*. https://doi.org/10.1176/appi.ajp.2010.09071059

Smith, S. M., Miller, K. L., Moeller, S., Xu, J., Auerbach, E. J., Woolrich, M. W., ... & Ugurbil, K. (2012). Temporally-independent functional modes of spontaneous brain activity. Proceedings of the National Academy of Sciences, 109(8), 3131-3136.

Sridharan, D., Levitin, D. J., & Menon, V. (2008). A critical role for the right fronto-insular cortex in switching between central-executive and default-mode networks. *Proceedings of the National Academy of Sciences of the United States of America*. https://doi.org/10.1073/pnas.0800005105

Tipper, S. P., Weaver, B., & Houghton, G. (1994). Behavioural Goals Determine Inhibitory Mechanisms of Selective Attention. *The Quarterly Journal of Experimental Psychology Section A*. https://doi.org/10.1080/14640749408401098

Todd, J., Michie, P. T., Budd, T. W., Rock, D., & Jablensky, A. V. (2000). Auditory sensory memory in schizophrenia: Inadequate trace formation? *Psychiatry Research*. https://doi.org/10.1016/S0165-1781(00)00205-5

Tsakanikos, E. (2004). Latent inhibition, visual pop-out and schizotypy: is disruption of latent inhibition due to enhanced stimulus salience?. Personality and Individual Differences, 37(7), 1347-1358.

Turetsky, B. I., Greenwood, T. A., Olincy, A., Radant, A. D., Braff, D. L., Cadenhead, K. S., Dobie, D. J., Freedman, R., Green, M. F., Gur, R. E., Gur, R. C., Light, G. A., Mintz, J.,

Nuechterlein, K. H., Schork, N. J., Seidman, L. J., Siever, L. J., Silverman, J. M., Stone, W. S., … Calkins, M. E. (2008). Abnormal Auditory N100 Amplitude: A Heritable Endophenotype in First-Degree Relatives of Schizophrenia Probands. *Biological Psychiatry*. https://doi.org/10.1016/j.biopsych.2008.06.018

Tustison, N. J., Cook, P. A., Holbrook, A. J., Johnson, H. J., Muschelli, J., Devenyi, G. A., Duda, J. T., Das, S. R., Cullen, N. C., Gillen, D. L., Yassa, M. A., Stone, J. R., Gee, J. C., & Avants, B. B. (2021). The ANTsX ecosystem for quantitative biological and medical imaging. *Scientific Reports*. https://doi.org/10.1038/s41598-021-87564-6

van Buuren, M., Vink, M., & Kahn, R. S. (2012). Default-mode network dysfunction and self-referential processing in healthy siblings of schizophrenia patients. Schizophrenia research, 142(1-3), 237-243.

Van Dijk, K. R., Hedden, T., Venkataraman, A., Evans, K. C., Lazar, S. W., & Buckner, R. L. (2010). Intrinsic functional connectivity as a tool for human connectomics: theory, properties, and optimization. Journal of neurophysiology, 103(1), 297-321.

Vatansever, D., Menon, D. K., Manktelow, A. E., Sahakian, B. J., & Stamatakis, E. A. (2015). Default mode dynamics for global functional integration. Journal of Neuroscience, 35(46), 15254-15262.

von Bastian, C. C., Belleville, S., Udale, R. C., Reinhartz, A., Essounni, M., & Strobach, T. (2022). Mechanisms underlying training-induced cognitive change. Nature Reviews Psychology, 1(1), 30-41.

Wan, L., Friedman, B. H., Boutros, N. N., & Crawford, H. J. (2008). P50 sensory gating and attentional performance. *International Journal of Psychophysiology*. https://doi.org/10.1016/j.ijpsycho.2007.10.008

Wang, X., Zhang, Y., Long, Z., Zheng, J., Zhang, Y., Han, S., Wang, Y., Duan, X., Yang, M., Zhao, J., & Chen, H. (2017). Frequency-specific alteration of functional connectivity density in antipsychotic-naive adolescents with early-onset schizophrenia. *Journal of Psychiatric Research*. https://doi.org/10.1016/j.jpsychires.2017.07.014

Weissman, D. H., Roberts, K. C., Visscher, K. M., & Woldorff, M. G. (2006). The neural bases of momentary lapses in attention. *Nature Neuroscience*. https://doi.org/10.1038/nn1727

Wen, X., Yao, L., Liu, Y., & Ding, M. (2012). Causal Interactions in Attention Networks Predict Behavioral Performance. *Journal of Neuroscience*. https://doi.org/10.1523/JNEUROSCI.2817-11.2012

Whitfield-Gabrieli, S., Thermenos, H. W., Milanovic, S., Tsuang, M. T., Faraone, S. V., McCarley, R. W., Shenton, M. E., Green, A. I., Nieto-Castanon, A., LaViolette, P., Wojcik, J., Gabrieli, J. D. E., & Seidman, L. J. (2009). Hyperactivity and hyperconnectivity of the default network in schizophrenia and in first-degree relatives of persons with schizophrenia. *Proceedings of the National Academy of Sciences of the United States of America*. https://doi.org/10.1073/pnas.0809141106

Winton-Brown, T. T., Fusar-Poli, P., Ungless, M. A., & Howes, O. D. (2014). Dopaminergic basis of salience dysregulation in psychosis. In *Trends in Neurosciences*. https://doi.org/10.1016/j.tins.2013.11.003

Won, G. H., Kim, J. W., Choi, T. Y., Lee, Y. S., Min, K. J., & Seol, K. H. (2018). Theta-phase gamma-amplitude coupling as a neurophysiological marker in neuroleptic-naïve schizophrenia. *Psychiatry Research*. https://doi.org/10.1016/j.psychres.2017.12.021

Wotruba, D., Michels, L., Buechler, R., Metzler, S., Theodoridou, A., Gerstenberg, M., Walitza, S., Kollias, S., Rössler, W., & Heekeren, K. (2014). Aberrant coupling within and across the

default mode, task-positive, and salience network in subjects at risk for psychosis. *Schizophrenia Bulletin*. https://doi.org/10.1093/schbul/sbt161

Wyatt, N., & Machado, L. (2013). Evidence Inhibition Responds Reactively to the Salience of Distracting Information during Focused Attention. *PLoS ONE*. https://doi.org/10.1371/journal.pone.0062809

Yan, C., Liu, D., He, Y., Zou, Q., Zhu, C., Zuo, X., ... & Zang, Y. (2009). Spontaneous brain activity in the default mode network is sensitive to different resting-state conditions with limited cognitive load. PloS one, 4(5), e5743.

Yee, C. M., Williams, T. J., White, P. M., Nuechterlein, K. H., Ames, D., & Subotnik, K. L. (2010). Attentional Modulation of the P50 Suppression Deficit in Recent-Onset and Chronic Schizophrenia. *Journal of Abnormal Psychology*. https://doi.org/10.1037/a0018265

Yeshurun, Y., & Carrasco, M. (1998). Attention improves or impairs visual performance by enhancing spatial resolution. *Nature*. https://doi.org/10.1038/23936

Zeidan, F., Martucci, K. T., Kraft, R. A., Gordon, N. S., Mchaffie, J. G., & Coghill, R. C. (2011). Brain mechanisms supporting the modulation of pain by mindfulness meditation. Journal of Neuroscience, 31(14), 5540–5548. https://doi.org/10.1523/JNEUROSCI.5791-10.2011

Zhou, L., Pu, W., Wang, J., Liu, H., Wu, G., Liu, C., Mwansisya, T. E., Tao, H., Chen, X., Huang, X., Lv, D., Xue, Z., Shan, B., & Liu, Z. (2016). Inefficient DMN Suppression in Schizophrenia Patients with Impaired Cognitive Function but not Patients with Preserved Cognitive Function. *Scientific Reports*. https://doi.org/10.1038/srep21657

Zhou, Y., Liang, M., Tian, L., Wang, K., Hao, Y., Liu, H., Liu, Z., & Jiang, T. (2007). Functional disintegration in paranoid schizophrenia using resting state fMRI. *Schizophrenia Research*. https://doi.org/10.1016/j.schres.2007.05.029